Journal of Integrative Neuroscience

J. Integr. Neurosci. **2026**; 25(4): 48640
https://doi.org/10.31083/JIN48640

Original Research

Involvement of the Primary Auditory Cortex-Basolateral Amygdala Circuit in Altered Conditioned Fear Memory Retrieval Following Electromagnetic Field Exposure in Mice

Zhilin Cui[1,2], Lei Shi[1], Meiying Yang[1], Chenxu Chang[1], Shunkang Jin[1], Yanhui Hao[1], Xuelong Zhao[1], Yanjie Lu[2], Yang Li[1,*], Hongyan Zuo[1,*]

[1]Department of Experimental Pathology, Beijing Institute of Radiation Medicine, 100850 Beijing, China
[2]Department of Pathophysiology, Chengde Medical University, 067000 Chengde, Hebei, China
*Correspondence: leeyoung109@hotmail.com (Yang Li); zuohy2005@126.com (Hongyan Zuo)
Academic Editor: Bettina Platt
Submitted: 28 November 2025 Revised: 2 February 2026 Accepted: 11 February 2026 Published: 17 April 2026

Abstract

Background: Electromagnetic field (EMF) exposure is increasingly common and has been implicated in a range of effects on human health. Conditioned fear memory plays a critical role in enabling organisms to respond appropriately to previously encountered threats. Despite growing interest in the neurobiological consequences of EMF exposure, its impact on the neural circuits underlying conditioned fear responses has not been clearly defined. **Methods**: Using a mouse model exposed to combined microwave and static magnetic fields, we examined the involvement of the primary auditory cortex-basolateral amygdala (Au1-BLA) circuit in EMF-associated alterations in conditioned fear retrieval. A multifaceted experimental approach was employed, including behavioral assays, viral tracing, genetically encoded calcium imaging, chemogenetic modulation, histopathological analysis, and immunofluorescence. **Results**: Exposure was associated with reduced conditioned fear memory retrieval, pathological changes in Au1 and BLA tissue ultra-structures, and decreased Nissl bodies in Au1 neurons and Au1-BLA neuronal fiber projections. The attenuation of conditioned fear memory retrieval coincided with decreased calcium activity in Au1 and BLA neurons. Consistently, chemogenetic activation of Au1 calcium-dependent protein kinase II (CaMKII)-expressing neurons enhanced calcium activity in BLA neurons during fear retrieval and was accompanied by changes in cholinergic signaling in the BLA. These findings suggest that cholinergic neuronal populations downstream of the Au1-BLA circuit are sensitive to EMF exposure and may participate in EMF-related modulation of fear retrieval. **Conclusions**: Our findings support an association between EMF exposure and altered conditioned fear expression involving functional changes within the Au1–BLA circuit, especially for the changes in calcium activity and chemogenetic modulation of Au1 CaMKII-expressing neurons. This study provides direct experimental evidence linking EMF exposure to circuit-level functional interactions underlying fear memory retrieval.

Keywords: fear conditioning; auditory cortex; amygdala; electromagnetic fields; neural pathways

1. Introduction

With the continuous advancement of global industrialization and informatization, the impact of electromagnetic radiation on human health has attracted increasing attention. Motor equipment, radar systems, and other devices often generate combined exposure to microwaves and static magnetic fields during operation, particularly in specialized occupational settings. In such environments, personnel working in proximity to radar installations or electromagnetic equipment may experience localized and time-dependent exposure to combined static magnetic fields and microwaves, whereas exposure levels in surrounding residential areas are generally much lower and subject to regulatory limits. According to the International Commission on Non-Ionizing Radiation Protection, the limit for public exposure to microwave radiation involving the head or trunk is a specific absorption rate (SAR) of 2 W/kg [1], and that for acute exposure to static magnetic fields involving any part of the body is 400 mT [2]. As previous studies have shown, exposure to a single static magnetic field and microwave radiation under certain conditions can lead to cognitive and behavioral disorders and anxiety-like behavior [3–5]. Electromagnetic field (EMF) exposure can impair fear memory capacity. Dehghani *et al*. [6] found that rats exhibited impaired fear extinction capacity after continuous exposure to 2.45 GHz radiofrequency radiation at a mean power density of 6 mW/cm^2 for 1 h per day over 7 days or 5–6 weeks. Additionally, as McKay *et al*. [7] reported, exposing rats to a static magnetic field of 0.5–1 mT to simulate the hippocampal theta rhythm impaired the acquisition and consolidation of contextual fear memory. However, the neurobiological effects of combined static magnetic field and microwave exposure have not been reported.

Fear memory is an adaptive response produced by organisms when facing dangerous environments, but its dysregulation is central to pathologies like post-traumatic stress disorder (PTSD) [8–10]. The formation of fear memory helps organisms effectively avoid danger when facing dan-

gerous environments again. Distinguishing between threatening and non-threatening stimuli is crucial for survival, and deficits in this discrimination are a core feature of PTSD. Auditory stimuli are usually applied for fear memory detection [11], partly because traumatic memories in humans are often linked to specific sounds, making it a highly relevant paradigm for translational research. Previous studies have shown that the auditory cortex not only processes auditory information but also participates in emotional learning and memory [12,13]. The primary auditory cortex (Au1) plays a key role in fear memory [13] as it is involved in identifying tone-emotion pairings and coordinating responses from other brain regions [14,15]. Additionally, the amygdala, particularly the basolateral amygdala (BLA), is a key brain region involved in the processing of emotions such as fear [16,17]. The BLA receives information from the auditory cortex, forms fear memories, and mediates defensive responses [18]. Furthermore, the extinction of fear memories is closely associated with the BLA [8,9,19]. Therefore, the Au1-BLA neural circuit plays an indispensable role in the fear memory process. However, the underlying molecular mechanisms of the Au1-BLA neural circuit are unclear.

In our previous studies, we found that exposure to a moderate static magnetic field of 100 mT (1 h/day for 7–14 days) induced neuroinflammatory responses in mice and disrupted dopamine-related signaling pathways [20,21]. In addition, microwave exposure at a SAR of 2.58 W/kg was shown to elicit anxiety-like behaviors and cause structural damage in the visual cortex of mice [22]. These findings provide experimental support for the use of a stable and biologically relevant animal model of combined EMF exposure. Based on this experimental framework, the present study employed a composite static magnetic field and microwave exposure paradigm to examine the effects of EMF exposure on conditioned fear memory expression and the associated neural processes within the Au1-BLA circuit. This study investigated the role of the Au1-BLA circuit in the conditioned fear memory after EMF exposure in mice, using conditioned fear memory behavioral tests, histopathological analysis, viral tracing, genetically encoded calcium indicators, chemical genetic regulation, and immunofluorescence. We analyzed changes in the morphological structure, neural fiber projections, and neuronal calcium activity in the Au1 and BLA brain regions in mice after EMF exposure and explored downstream target neurons in the Au1–BLA circuit, as well as their potential regulatory roles. Collectively, this study aims to provide experimental evidence on how EMF exposure may interact with neural circuits underlying fear-related behavior, while clarifying the scope and limitations of the circuit-level associations observed under the present experimental conditions.

2. Materials and Methods

2.1 Animals and Groups

All animal procedures were approved by the Institutional Animal Care and Use Committee of the Beijing Institute of Radiation Medicine (Protocol No. IACUC-DWZX-2021-685). Ten-week-old wild-type C57BL/6N mice (SPF Biotechnology Co., Ltd, Beijing, China) weighing 22–24 g, with an equal number of males and females, were housed at the Experimental Animal Center of the Beijing Institute of Radiation Medicine. Mice were randomly divided into a control group (Con), static magnetic field exposure group (MF), microwave exposure group (MW), and static magnetic field and microwave exposure group (MF&MW). All mice were housed in an environment maintained at 18–22 °C, relative humidity of 50–60%, and a 12:12 h light-dark cycle, with free access to food and water.

2.2 EMF Exposure

Animals were placed in a transparent, perforated acrylic box which allowed free movement, and their whole body was exposed to EMF. For static magnetic field exposure, mice were placed in a uniform field 1 cm away from the center of the magnetic field, with a field intensity of 100 mT, for 1 h (Fig. 1A). For microwave exposure, mice were placed on a platform, 43 cm away from the transmitter antenna, with a center frequency of 9.375 GHz and an average power density of 12 mW/cm^2, for 15 min (Fig. 1B). Electromagnetic dosimetry was performed using a finite-difference time-domain algorithm implemented in the Sim4Life platform (ZMT Zurich MedTech AG, Zurich, Switzerland), incorporating a mouse-specific anatomical model (Diggy Male Nude Normal Mouse Model, 23.3 g). Both the exposure antenna and mouse geometry were explicitly modeled to calculate whole-body and spatial SAR distributions under the experimental exposure conditions. Whole-body averaged SAR values ranged from 2.33 to 2.83 W/kg across individual mice (mean, 2.58 W/kg). Under rotation around the platform center during exposure, absorbed dose was considered comparable across animals. Simulated SAR distributions showed no evidence of focal hotspots (**Supplementary Fig. 1A**). To directly assess potential thermal effects during EMF exposure, rectal temperature of mice was monitored using optical fiber thermometry. Rectal temperature was recorded for 5 min prior to exposure to establish baseline values, continuously monitored throughout the 15-min microwave exposure period, and further measured for 5 min following the end of exposure. No significant elevation in rectal temperature was observed during or after EMF exposure (**Supplementary Fig. 1B**). The control group mice were placed in the same acrylic box under the same experimental conditions, exposed for the same duration, but without a static magnetic field and microwave exposure. Mice in the MF group were exposed only to the static magnetic field, whereas those in the MW group were exposed only to microwaves. Mice in the com-

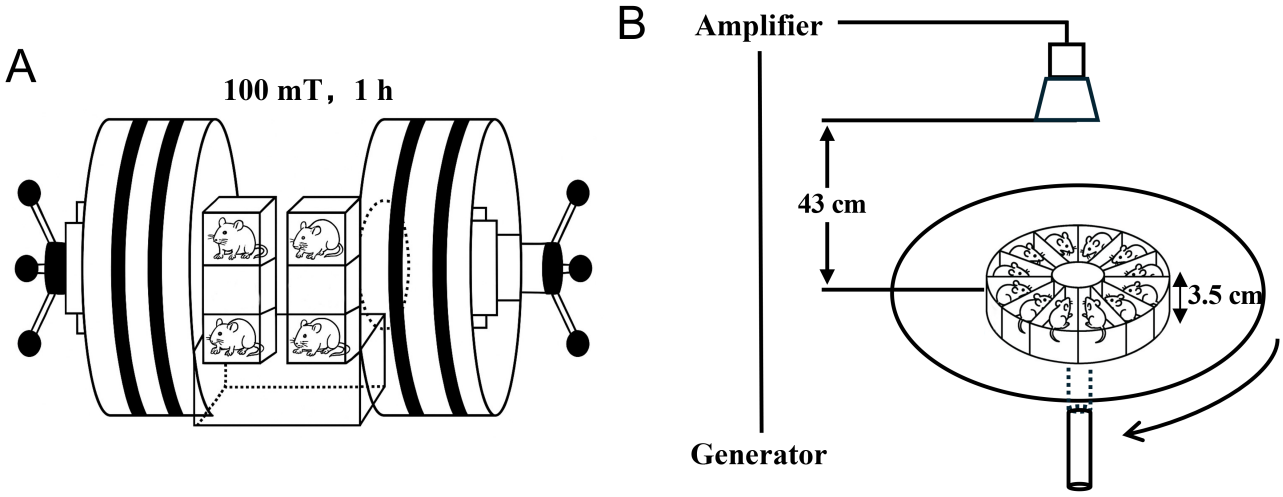

Fig. 1. Diagram of electromagnetic field exposure system. (A) Static magnetic field exposure. (B) Microwave exposure.

bined exposure group were exposed to microwaves after exposure to a static magnetic field.

2.3 Conditional Fear Memory Test

The conditioned fear memory test was conducted using the Conditioned Fear Memory System (NIR-022; Med Associates Inc., St. Albans, VT, USA). The experiment was divided into two stages: fear memory training (training) and fear memory testing (retrieval-based test). Two sound stimuli with frequencies of 12 and 2 kHz were selected, both with an intensity of 75 dB. During the training phase, mice were placed in the fear chamber for 150 s for acclimation. The two kinds of sound stimuli were presented in a pseudo-random manner, with a duration of 20 s for each stimulus and a 30-s interval between stimuli. Each of the two sound stimuli was presented 10 times. The 12 kHz stimulus was paired with an electric foot shock of 0.6 mA intensity during the last 2 s of sound duration. The 2 kHz stimulus was presented without a paired electric foot shock. Each mouse was taken out of the fear chamber 2 min after the last sound stimulation and the experiment was repeated with the next mouse. The testing phase was designed to assess the retrieval of an already established conditioned fear memory. After a period of 150 s to allow the mouse to adapt to the fear chamber, mice were presented with a 12 kHz tone lasting 100 s without foot shock, followed by removal from the chamber 2 min later. After a 2-h interval, mice were placed in the fear chamber again, and a 2 kHz sound stimulus was administered, lasting 100 s. Freezing behavior during tone presentation was quantified as an index of conditioned fear memory expression. The duration of freezing response for each mouse was measured 1 s after the onset of continuous freezing behavior, and the percentage of freezing time during the sound stimulation was calculated. Freezing was defined as complete immobility, excluding breathing.

2.4 Auditory Function Assessment

2.4.1 Auditory Brainstem Response (ABR)

ABRs were measured to assess hearing sensitivity in mice. Animals were anesthetized by intraperitoneal injection of sodium pentobarbital (Cat. No. YU021, Shanghai Yuyan Scientific Instruments Co., Ltd., Shanghai, China) (1%, 100 mg/kg). After anesthesia, mice were placed in a sound-attenuated and electrically shielded chamber. ABR recordings were performed using a standard auditory evoked potential system (SmartEP-M010000, Intelligent hearing Systems, Miami, FL, USA). Recording electrodes were inserted subcutaneously near the bilateral pinnae, with the ground electrode placed subcutaneously at the midpoint between the two ears on the scalp. Acoustic stimuli were delivered through a sound delivery tube positioned in the external auditory canal. Click stimuli were used for ABR acquisition. Signals were averaged over 1024 sweeps with a total analysis window of 10 ms. Stimulation intensity started at 90 dB sound pressure level (SPL) and was decreased in 10 dB SPL steps to 50 dB SPL, followed by 5 dB SPL decrements until wave I was no longer detectable. The lowest stimulus intensity at which a reproducible ABR wave I could be identified was defined as the hearing threshold. ABR thresholds were recorded for both ears.

2.4.2 Distortion Product Otoacoustic Emissions (DPOAE)

Following ABR measurements, DPOAE were recorded to evaluate cochlear outer hair cell function. DPOAE testing was conducted using a dedicated otoacoustic emission analysis system. An ear probe was gently inserted into the external auditory canal of each mouse. Two primary tones (f1 and f2) were presented simultaneously, with sound pressure levels of 65 dB SPL for f1 and 55 dB SPL for f2. The resulting distortion product at the frequency of 2f1–f2 was recorded. Measurements were obtained across frequencies ranging from 0.5 to 32 kHz.

DPOAE amplitude was collected for both ears at each frequency point and used for subsequent analysis.

2.5 Histopathological Analysis

The structural organization of the brain underlies its functioning. Previous behavioral test showed a decline in conditioned fear memory at 7 days after EMF exposure. Thus, the morphological changes in the Au1 and BLA brain regions, which are closely related to conditioned fear memory, were observed by transmission electron microscopy at 7 days after EMF exposure.

Mice were anesthetized with 1% pentobarbital sodium (Cat. No. YU021, Shanghai Yuyan Scientific Instruments Co., Ltd., Shanghai, China) (50 mg/kg) via intraperitoneal injection, followed by cardiac perfusion with 4% paraformaldehyde for fixation. The brain tissue was then harvested. For Nissl staining, the brain tissue was rapidly placed in a 4% paraformaldehyde solution (Cat. No. P4500, Sinopharm Chemical Reagent Co., Ltd., Shanghai, China) for one-week fixation, and then dehydrated with graded ethanol, cleared in xylene (Cat. No. CAS 1330-20-7, Sinopharm Chemical Reagent Co., Ltd., Shanghai, China) and embedded in paraffin. Coronary sections (3-µm thick) of the auditory cortex and amygdala regions were made. The sections were dewaxed with xylene, dehydrated with graded ethanol, and stained with 0.5% toluidine blue solution (Cat. No. BL999A, Biosharp, Hefei, Anhui, China) at room temperature for 25 min. After differentiation with 70% ethanol, xylene transparency, and neutral-resin mounting, the sections were observed using an optical microscopy system (DX12; 3DHISTECN, Budapest, Hungary). Image analysis was performed using ImageJ (2024, Fiji 1.54f) software (NIH, Bethesda, MD, USA) to calculate the mean optical density (MOD) of Nissl bodies.

For ultrastructural morphology, the left Au1 and amygdala were dissected on ice, placed in 2.5% glutaraldehyde (Cat. No. CAS 111-30-8; Xiamen Haibiao Technology Co., Ltd., Xiamen, China) for 2 h, followed by fixation with 1% osmic acid (Cat. No. O109047, Aladdin Bio-Chem Technology Co., Ltd., Shanghai, China) for 2 h, dehydrated with graded ethanol and acetone (Cat. No. A475456, Aladdin Bio-Chem Technology Co., Ltd., Shanghai, China), embedded in Epon 812, and after positioning the semi-thin sections, ultra-thin sections were prepared. Then double staining with uranium acetate and lead citrate was performed, and the ultrastructural morphologies were observed using a transmission electron microscope (HT-7800; Hitachi, Tokyo, Japan).

For influence observation, the frozen sections of brain were prepared using a cryostat (CM1950; Leica, Wetzlar, Germany) with a thickness of 20 µm. After mounted with an anti-fluorescence quenching mounting medium (containing DAPI) (104139, Abcam, Cambridge, UK), the sections were observed using a laser scanning confocal microscope (LSM880; Leica, Germany). Quantitative analysis of the fluorescent images was performed using ImageJ software (Fiji, version 1.54f, NIH, Bethesda, MD, USA), and the relative fluorescent area (area %) was calculated.

2.6 Stereotactic Injection of Virus

The viruses used included rAAV-hSyn-EGFP (Cat. No. BC-0020, BrainCase Biotechnology Co., Ltd., Shenzhen, Guangdong, China), rAAV-hSyn-mCherry (Cat. No. BC-0023, BrainCase Biotechnology Co., Ltd.), rAAV-hSyn-jGCaMP7b (Cat. No. BC-0258, BrainCase Biotechnology Co., Ltd.), rAAV-CaMKIIα-hM3D(Gq)-EGFP (Cat. No. BC-0139, BrainCase Biotechnology Co., Ltd.), and rAAV-CaMKIIα-hM4D(Gi)-EGFP (Cat. No. BC-0245, BrainCase Biotechnology Co., Ltd.). Mice were anesthetized by inhalation of 4–5% isoflurane (Cat. No. R510-22-2, Ruiwode Life Science Co., Ltd.) and fixed in a stereotaxic apparatus (Cat. No. 68025, Ruiwode Life Science Co., Ltd.). Erythromycin ointment (Cat. No. H36020018, Jiangxi Decheng Pharmaceutical Co., Ltd., Nanchang, Jiangxi, China) was applied for eye protection, and a heating pad was used to maintain body temperature at 37 °C. After disinfection, the scalp was removed to expose the skull. A mini drill was used to drill holes into the skull, and the virus was injected into the target brain region at a rate of 30 nL/min via a glass micro-needle using a microsyringe pump. The coordinates for Au1 and BLA were determined based on the mouse brain atlas: Au1 (anterior-posterior (AP): –2.3 mm, medial-lateral (ML): ±4.3 mm, dorsal-ventral (DV): –3.2 mm) and BLA (AP: –1.2 mm, ML: ±3.8 mm, DV: –4.9 mm). After injection, the needle was left for 10 min. Following removal of the needle, dental cement was applied. The mouse was then allowed to awaken naturally before being returned to its housing cage for recovery.

To detect calcium activity in Au1 and BLA neurons, rAAV-hSyn-jGCaMP7b was injected into the Au1 and BLA of mice and ceramic inserts were implanted at the virus injection sites. To detect Au1-BLA neuronal fiber projections, rAAV-hSyn-EGFP was injected into the Au1, and rAAV-hSyn-mCherry was injected into the BLA. To regulate the activity of Au1 glutamatergic neurons, rAAV-CaMKIIα-hM3D(Gq)-EGFP or rAAV-CaMKIIα-hM4D(Gi)-EGFP was injected into the Au1.

2.7 Genetically Encoded Calcium Imaging

Three weeks after AAV-jGCaMP7b injection into the Au1 and BLA, the conditioned fear memory test was conducted. A fiber-optic recording system (QAXK-FPS-SS-MC-LED, Thinker Tech Nanjing Bioscience Inc., Nanjing, China) was used to continuously record neuronal calcium activity throughout the entire behavioral session. The fiber-optic patch was inserted through a small hole above the fear chamber and connected to the ceramic implant in the mouse. A 473-nm laser was delivered through the optical fiber to excite the genetically encoded calcium indicator jG-

CaMP7b, and fluorescence signals were continuously acquired during the entire sound stimulation period, including both freezing and non-freezing behavioral states.

To characterize neural activity associated with fear expression, freezing onset was identified based on frame-by-frame behavioral scoring. For freezing-aligned analyses, calcium traces were aligned to the onset of each freezing episode. The local trough immediately preceding the rise of the calcium signal waveform was defined as the reference time point (T = 0 s) for visualization of freezing-associated calcium dynamics. Calcium signals were expressed as $\Delta F/F_0 = (F_{signal} - F_0)/F_0$, where F_0 was calculated as the mean fluorescence value during the –2 to 0 s baseline period preceding T = 0 s. In addition, to assess stimulus-evoked calcium responses independent of behavioral state, a separate tone-onset-locked analysis was performed. In this analysis, time zero was defined as the onset of the auditory stimulus (100 s sound onset), and calcium signals were extracted within a –2 to +10 s window relative to tone onset for both the 12 kHz conditioned tone and the 2 kHz non-conditioned tone. All trials were included regardless of subsequent freezing behavior. Data analysis was performed using MATLAB (Version R2024a, MathWorks, Natick, MA, USA).

2.8 Chemical Genetic Regulation

Three weeks after injection of AAV-CaMKIIα-hM3D or AAV-CaMKIIα-hM4D, mice received an intraperitoneal injection of either saline (NS) or clozapine-N-oxide (Cat. No. CNO-25 mg, BrainCase Biotechnology Co., Ltd., Shenzhen, Guangdong, China), prepared at 0.33 mg/mL and administered at a volume of 0.01 mL/g body weight (approximately 3.3 mg/kg), 30 min prior to behavioral testing. CNO administration was used to modulate the activity of Au1 CaMKIIα-expressing excitatory neurons expressing designer receptors exclusively activated by designer drugs, whereas saline served as a vehicle control. Following these manipulations, conditioned fear behavioral tests were conducted, and freezing behavior during sound stimulation was quantified to assess changes in fear retrieval.

2.9 Immunofluorescence Staining

Double immunofluorescence staining was used to detect the expression of neuronal-specific markers (ChAT and GAD 67) and c-Fos was used as a neuronal activity marker. Briefly, frozen sections of brain tissue were treated with 0.25% Triton X-100 for 25 min, followed by antibody blocking with 1% bovine serum albumin (BSA) (Cat. No. A8020, Solarbio Science & Technology Co., Ltd., Beijing, China) for 2 h. Then, the mixture diluent of c-Fos antibody (1:1000, Cat. No. 2250, Cell Signaling Technology, Danvers, MA, USA) and GAD 67 (1:1000, Cat. No. ab26116, Abcam, Cambridge, UK) antibody, or c-Fos antibody (1:200, Cat. No. ab208942, Abcam) and ChAT (1:1000, Cat. No. ab6168, Abcam) antibody diluent was added and the sections were incubated at 4 °C overnight. After washing three times with 0.025% Triton X-100 (Cat. No. G3068, Wuhan Servicebio Technology Co., Ltd., Wuhan, Hubei, China) in phosphate-buffered saline (PBS) (Cat. No. G4202, Wuhan Servicebio Technology Co., Ltd.), a mixture of goat anti-rabbit (1:500, Cat. No. Alexa Fluor® 488, Abcam) and goat anti-mouse (1:500, Cat. No. Alexa Fluor® 594, Abcam) secondary antibody was added and the sections were incubated at room temperature for 2 h, followed by washing with 0.025% Triton X-100 in PBS.

After mounting with anti-fluorescence quencher medium, the sections were observed using a laser scanning confocal microscope (LSM880; Leica, Wetzlar, Germany). Quantitative analyses were performed with ImageJ software. For each section, regions of interest (ROIs) corresponding to the BLA were manually delineated according to anatomical landmarks. Following background subtraction and thresholding with identical parameters across groups, the fluorescence-positive areas for c-Fos and for ChAT or GAD67 were measured independently. To estimate relative neuronal activity within specific cell populations, cholinergic and GABAergic activity indices were calculated as the ratio of c-Fos-positive area to ChAT-positive area (Area-c-Fos/Area-ChAT) or to GAD67-positive area (Area-c-Fos/Area-GAD67), respectively. In parallel, fluorescence colocalization was assessed using the Colocalization Finder plugin in ImageJ. Pearson's correlation coefficients were calculated to quantify the spatial association between c-Fos and ChAT signals, or between c-Fos and GAD67 signals, within the defined ROIs.

2.10 Statistical Analysis

All experimental data were reported as the mean and standard error of the mean (SEM). Statistical analysis was performed using SPSS 27.0 software (IBM Corp., Armonk, NY, USA). Core body temperature measurements obtained before, during, and after EMF exposure were analyzed using paired two-tailed Student's *t*-tests. The conditioned fear memory behavior was analyzed using two-way repeated-measures ANOVA. For sex-stratified analyses and DPOAE amplitude data were additionally analyzed using multivariate ANOVA with sex and exposure condition as between-subject factors. Quantification data of Nissl staining and immunofluorescence staining were analyzed using two-way ANOVA. The statistical significance of differences in ABR thresholds, neural-fiber projection, and neuronal calcium signals between groups was assessed using independent samples *t*-tests. p values < 0.05 were considered statistically significant.

3. Results

3.1 Attenuation of Conditioned Fear Memory Retrieval Following EMF Exposure

Fear memory is one of the most important emotions in both humans and animals, and is generally associated with cues such as sound or light stimuli [23]. This study used Pavlov's classical conditioning model to associate auditory stimuli with foot shock, testing the discrimination of two sounds with different frequencies, and the freezing response in mice. A behavioral paradigm of fear discrimination during retrieval-based testing was established for EMF exposure as shown in Fig. 2A,B.

During the conditioned fear training phase, freezing behavior progressively increased and exceeded 80% from the sixth to tenth tone presentation, indicating successful acquisition of conditioned fear memory prior to EMF exposure (Fig. 2C). During the test phase, behavioral responses were evaluated at multiple post-exposure time points to assess the retrieval of conditioned fear memory. At 6 h after exposure, the percentage of freezing time response to 2 kHz stimulus was lower in the MF&MW group than in the MF group 6 h (Fig. 2D). The percentage of freezing time in response to 12 kHz stimulus with electric shock 7 d after EMF exposure was significantly lower in the MF&MW group than in the other groups (Fig. 2E). The percentage of freezing time in response to a 2 kHz stimulus without electric shock was also significantly higher in the MF&MW group than in the other groups (Fig. 2F). The ratio of 2:12 kHz freezing time percentage, percentage of freezing time of 12 kHz after 6 h, and the freezing time percentage 14 days after exposure did not differ significantly between groups (**Supplementary Fig. 2**). These results indicate that combined exposure was associated with reduced retrieval of conditioned fear in mice, with the difference being most apparent at 7 days after exposure, whereas exposure to MF or MW alone did not result in detectable changes in fear-related behavior under the present conditions.

To evaluate whether the EMF-associated alterations in conditioned freezing behavior could be attributed to peripheral auditory dysfunction, auditory function was assessed using ABR and DPOAE. ABR testing revealed no significant differences in auditory thresholds among Con, MF, MW, and MF&MW group at 7 days post-exposure, in either the left or right ear (Fig. 3A,B). These results indicate that EMF exposure did not induce detectable impairments in auditory nerve or brainstem function. In line with these findings, DPOAE recordings revealed no significant group differences in distortion product amplitudes across the tested frequency range in either ear (Fig. 3C,D), suggesting preserved outer hair cell function following EMF exposure. Together, these findings indicate that the attenuation of conditioned freezing behavior observed following EMF exposure is unlikely to result from gross auditory dysfunction and instead supports an interpretation based on altered conditioned fear retrieval rather than primary sensory deficits.

Because sex differences have been reported in fear related behaviors [24,25], we next examined whether EMF exposure induced changes in freezing responses differed between male and female mice. The results showed a significant effect of exposure condition on freezing responses at 7 days after EMF exposure, whereas no sex-related differences or sex-by-exposure interactions were observed for freezing responses to the 12 kHz conditioned stimulus, the 2 kHz non-conditioned stimulus, or the 2:12 kHz freezing ratio (**Supplementary Fig. 3D–F**). In contrast, no significant effects of sex or sex-by-exposure interactions were detected at 6 h (**Supplementary Fig. 3A–C**) or 14 days (**Supplementary Fig. 3G–I**) after EMF exposure for any of the measured fear-related indices. These results indicate that the EMF-associated attenuation of conditioned fear retrieval observed at the 7-day time point was comparable between male and female mice under the present experimental conditions.

3.2 Pathological Changes in Au1 and BLA After EMF Exposure in Mice

Ultrastructure observation 7 days after EMF exposure revealed irregular nuclei, nuclear chromatin condensation and margination, indistinct nuclear membrane, focal vacuolization of swollen mitochondria, and dilation and degranulation of endoplasmic reticulum in some Au1 and BLA neurons. Moreover, blurring of the synaptic clefts, loss of definition of the double membranes, and accumulation of synaptic vesicles in the presynaptic terminal were observed in the EMF exposure groups (Fig. 4A,B). These pathological changes of ultrastructure were more marked in the MF&MW group than in the MF and MW groups, and the changes were more marked in Au1 neurons than in BLA neurons. This suggests that EMF exposure can cause pathological changes of ultrastructure in neurons in the Au1 and BLA regions of mice.

The effects of EMF exposure on neurons in the Au1 and BLA regions, were confirmed by investigating the changes of Nissl body in neurons by Nissl staining for both Au1 and BLA 7 days after EMF exposure (Fig. 4C). This revealed a significant reduction in the MOD of Nissl bodies in the Au1 neurons in the MF&MW group, compared with those in the Con group, whereas the MOD of Nissl bodies in the Au1 neurons in the MF and MW groups did not differ significantly from that of the Con group (Fig. 4D). The MOD of Nissl bodies in the BLA neurons in the MF&MW, MF, and MW groups also did not differ significantly from that of the Con group (Fig. 4E). The reduction in the MOD of Nissl bodies indicates a decrease in the amount of rough endoplasmic reticulum and free ribosomes within neurons, suggesting that EMF exposure may inhibit the protein synthesis in Au1 neurons. Additionally, the results of Nissl body staining suggest that the effects of EMF exposure on

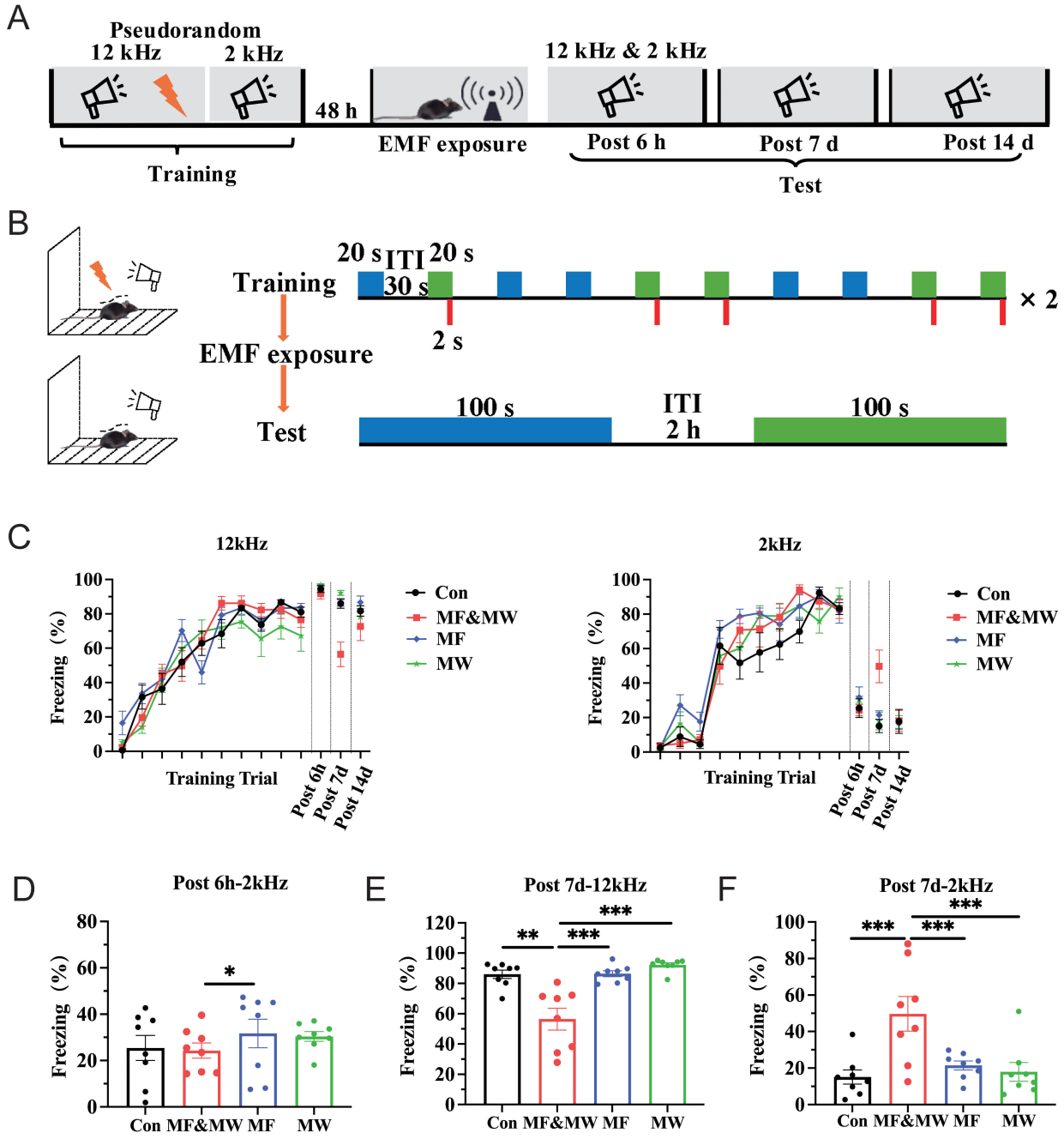

Fig. 2. Electromagnetic field exposure attenuates conditioned fear memory retrieval in mice. (A) Timeline of conditioned fear memory experiment. (B) Schematic diagram of the auditory fear conditioning and retrieval-based testing procedure. (C) Percentage of freezing time in mice for each group during the conditioned fear memory training and retrieval-based test phases. (D) Percentage of freezing time response to 2 kHz sound stimulus 6 h after exposure. (E,F) Percentage of freezing time response to 12 kHz (E) and 2 kHz (F) sound stimulus 7 days after exposure. Mean ± SEM, n = 8, two-way repeated-measures ANOVA. *$p < 0.05$, **$p < 0.01$, ***$p < 0.001$. Con, control group; MF, static magnetic field exposure group; MF&MW, combined static magnetic field and microwave exposure group; MW, microwave exposure group.

Au1 neurons were more pronounced than those on the BLA neurons, and that the combined exposure of MF&MW had a more marked effect on Au1 neurons than either MF or MW exposure alone.

3.3 Alteration of Au1-BLA Neural Projection Intensity After EMF Exposure

Au1 is responsible for processing auditory stimuli related to emotions and transmitting the information to the BLA [26,27]. Therefore, this study investigated the ef-

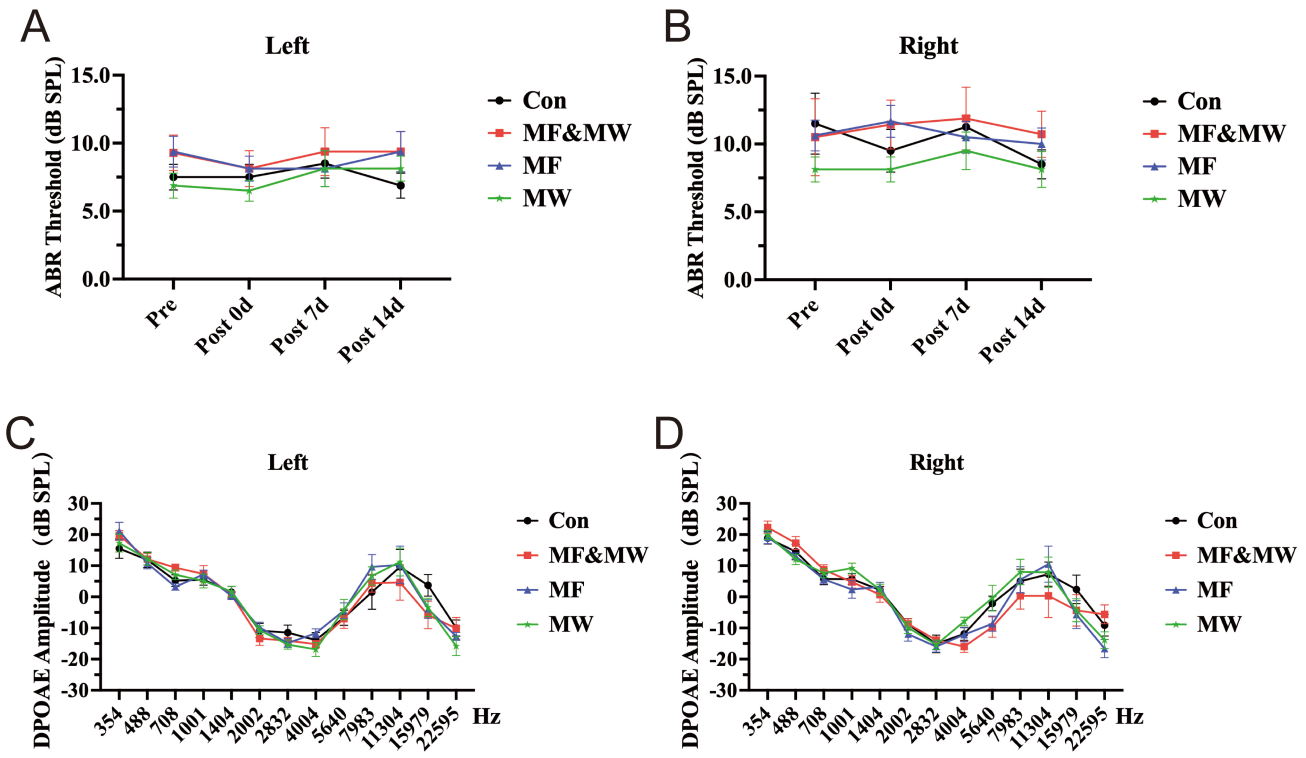

Fig. 3. Changes of ABR thresholds and DPOAE assessments in mice after electromagnetic field exposure. (A,B) ABR thresholds measured in the left (A) and right (B) ears of mice in all experimental groups at multiple time points (Pre, Post 0 d, Post 7 d, and Post 14 d) after exposure. (C,D) Changes in DPOAE amplitudes in the left (C) and right (D) ear of mice from each experimental group at 7 days after exposure. Mean ± SEM, n = 8, ABR: *t*-test; DPOAE: multivariate ANOVA.

fects of EMF exposure on the Au1-BLA neural projections by anterograde and retrograde tracing. For anterograde tracing, rAAV2/9-hSyn-EGFP-WPRE-hGHpA was injected into the Au1. For retrograde tracing, rAAV2/retro-hSyn-mCherry-WPRE-hGHpA was injected into the BLA.

The accuracy of the micro-injection was confirmed by the expression of fluorescent protein EGFP or mCherry (Fig. 5A,B). The quantification of Au1-BLA projection (Fig. 5C,D) showed that 7 days after exposure, both the anterograde (Fig. 5E) and retrograde (Fig. 5F) projections were significantly reduced in the MF&MW group compared with the Con group. These findings indicate that EMF exposure is associated with a reduction in projection-consistent labeling along the Au1-BLA pathway, suggesting an altered functional state of the Au1-BLA circuit under EMF exposure. Rather than indicating a definitive loss of anatomical connectivity, this change is more likely to reflect alterations in activity-dependent labeling efficiency or functional properties of Au1-BLA projections.

3.4 Reduced Calcium Activity in Au1 and BLA Neurons is Associated With Altered Conditioned Fear Memory Expression in Mice Exposed to EMF

Au1 is responsible for the integration and transmission of auditory information [12], whereas BLA processes and stores emotional information and coordinates behavior [9,28]. Both Au1 and BLA play an important role in conditioned fear memory [29]. To investigate the neural mechanisms underlying the attenuation of conditioned fear expression following combined exposure to static magnetic fields and microwaves, we used genetically encoded calcium imaging technology, rAAV-hSyn-jGCaMP7b were injected into the Au1 and BLA brain regions (Fig. 6A). Using fiber-optic recordings combined with conditioned fear memory behavioral tests, we examined calcium activity in Au1 and BLA neurons during the retrieval phase of conditioned fear memory. Calcium signals were first analyzed time-locked to the onset of auditory stimulation, independent of behavioral state. We then analyzed calcium activity in Au1 and BLA neurons during sound-evoked freezing episodes in the conditioned fear memory test, focusing on neural activity associated with fear expression (Fig. 6B).

Seven days after EMF exposure, tone-onset–aligned analysis revealed no significant differences in stimulus-evoked calcium responses between the MF&MW and control groups, either during presentation of the fear-paired 12 kHz tone or the non-paired 2 kHz tone (**Supplementary Fig. 4**), indicating that EMF exposure did not alter the immediate neural response to auditory cue onset. In contrast, when calcium signals were analyzed during freezing episodes elicited by the fear-paired 12 kHz tone, a significant reduction in calcium activity was observed in both Au1

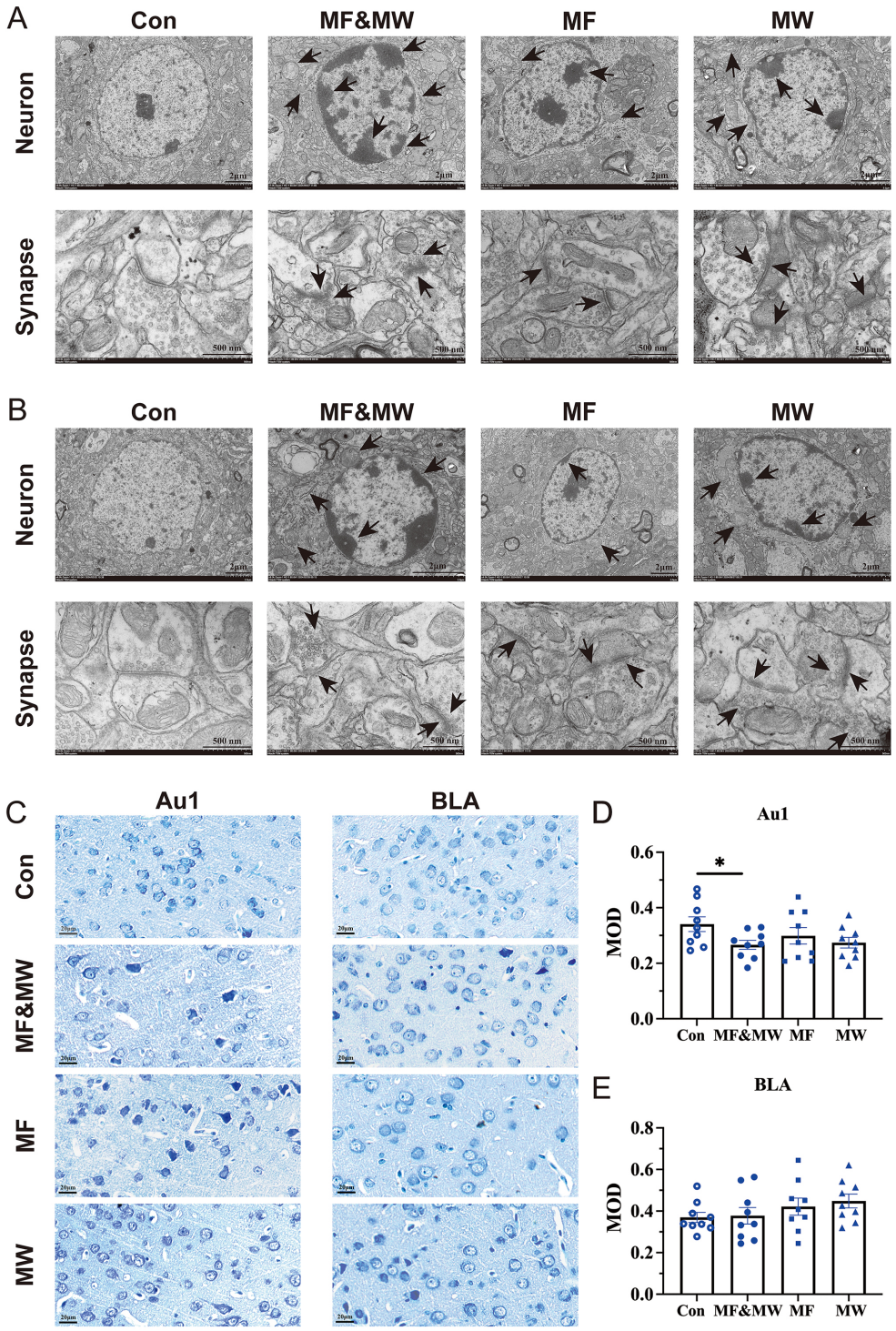

Fig. 4. Pathological changes of the Au1 and BLA neurons in mice exposed to electromagnetic radiation. (A,B) Ultrastructure of neurons and synapses in the Au1 (A) and BLA (B), Black arrows indicate representative pathological features, including cytoplasmic condensation along the nuclear membrane, mitochondrial swelling, accumulation of synaptic vesicles, and blurred synaptic clefts. (C) Representative images of Nissl body staining in Au1 and BLA. (D,E) Quantification of Nissl body in the Au1 (D) and BLA (E). Mean ± SEM, n = 6, Two-way ANOVA. *$p < 0.05$. Au1, primary auditory cortex; BLA, basolateral amygdala; Con, control group; MF, static magnetic field exposure group; MF&MW, combined static magnetic field and microwave exposure group; MOD, mean optical density; MW, microwave exposure group. Scale bars: Neurons, 2 μm; Synapses, 500 nm (A,B); 20 μm (C).

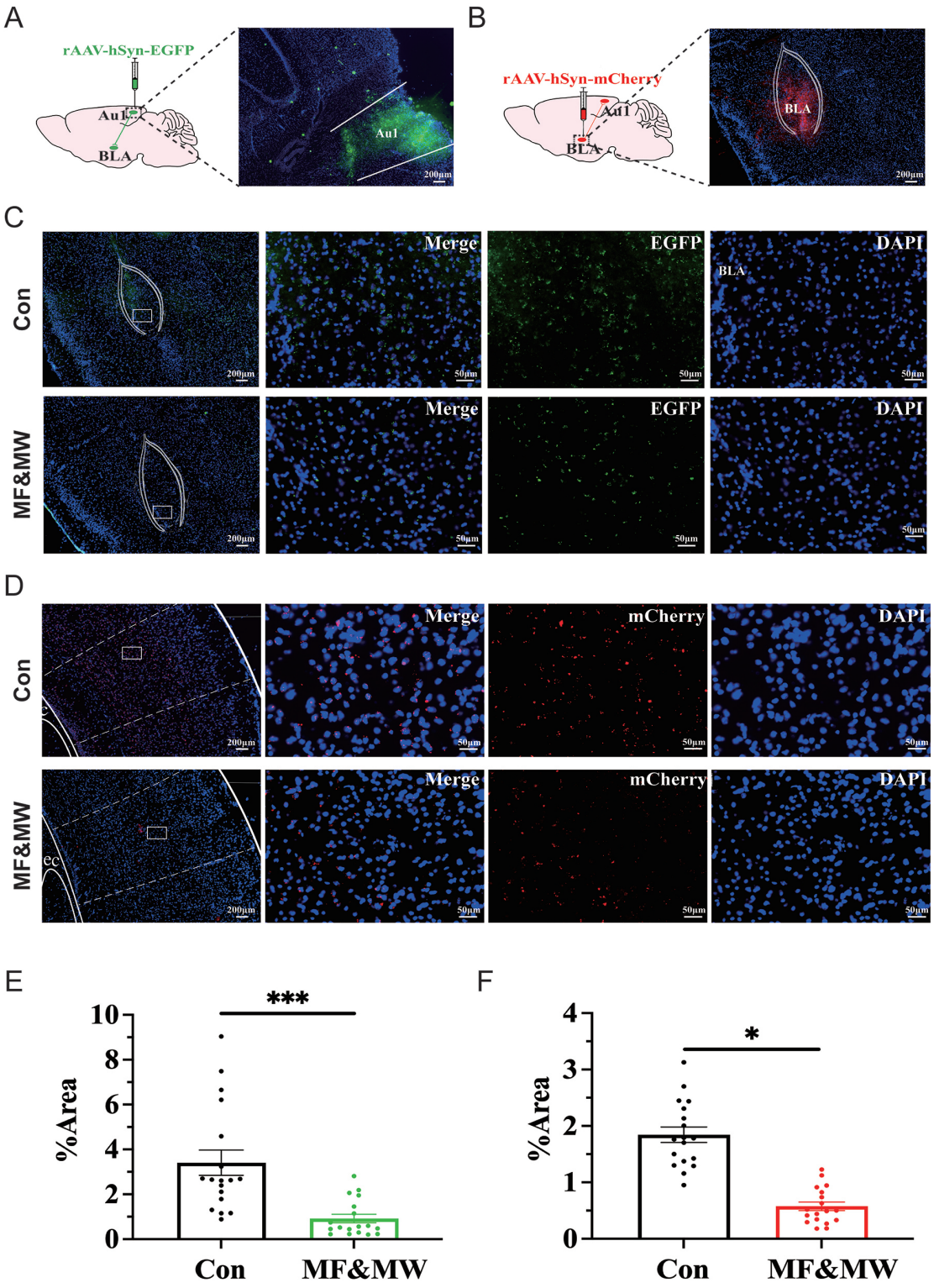

Fig. 5. Electromagnetic field exposure is associated with altered Au1-BLA projection intensity. (A,B) Confirmation of the target region Au1 (A) and BLA (B) for micro-injection of rAAV-hSyn-EGFP and rAAV-hSyn-mCherry, respectively. (C,D) Representative images of BLA (C) and Au1 (D) for the Au1-BLA projections by AAV-based tracing. (E,F) Quantification analysis of the Au1-BLA projections by anterograde (E) and retrograde (F) AAV-based tracing. Mean ± SEM, n = 6, independent samples *t*-test. *$p < 0.05$, ***$p < 0.001$. AAV, adeno-associated virus. Scale bars: 200 μm (A, B, and low-magnification images in C and D); 50 μm (high-magnification images in C and D).

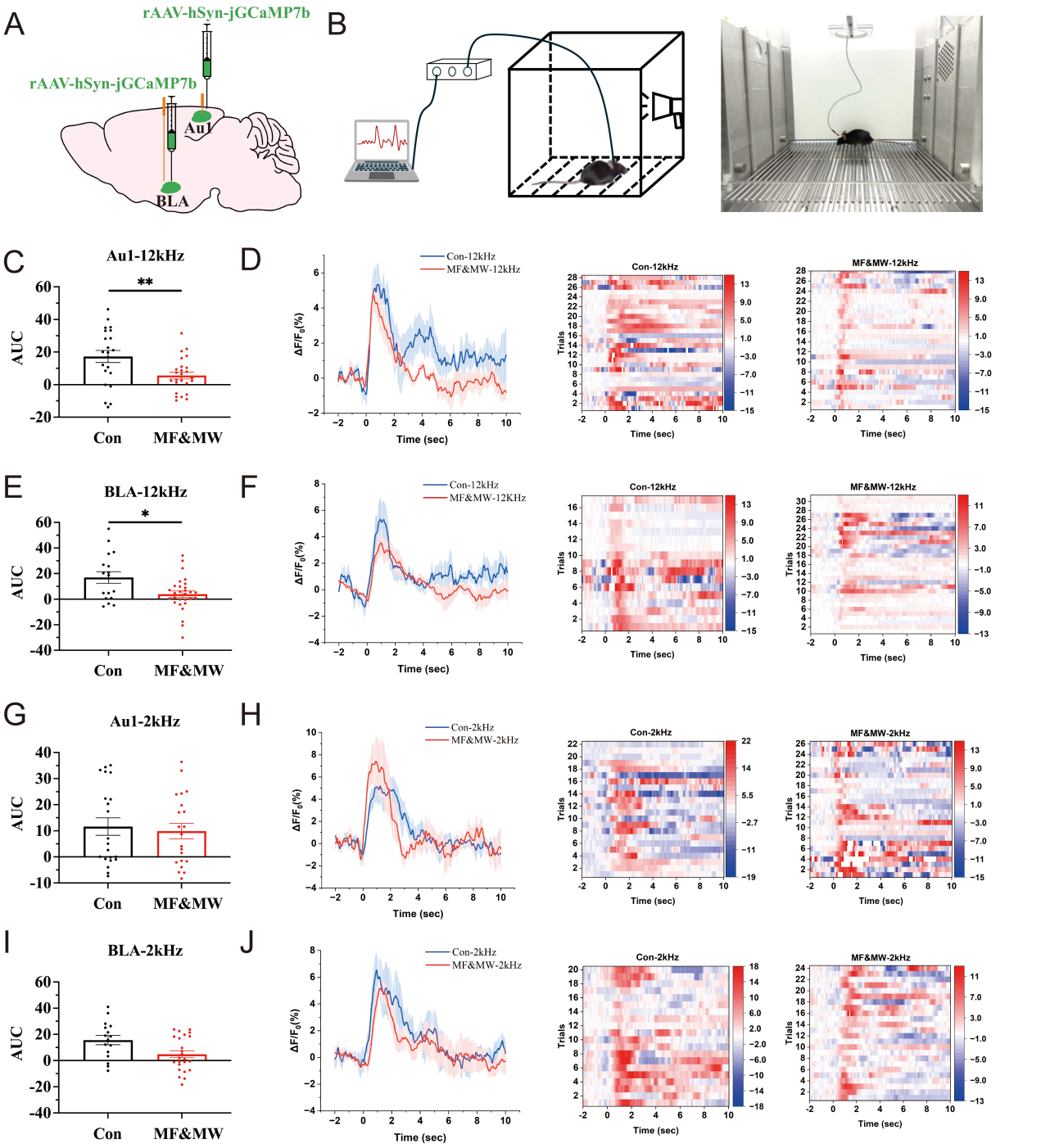

Fig. 6. Reduced calcium activity in Au1 and BLA neurons is associated with impaired conditioned fear memory retrieval in mice exposed to electromagnetic fields. (A) Schematic diagram of rAAV-GCaMP injection into the Au1 and BLA brain regions. (B) Schematic diagram of fiber optic recording combined with conditioned fear memory tests. (C–F) Plot of AUC, $\Delta F/F_0$ (%), and heat maps of calcium signal in the Au1 (C,D) and BLA (E,F) during conditioned fear retrieval elicited by the 12 kHz tone. (G–J) Plot of AUC, $\Delta F/F_0$ (%), and heat maps of calcium signal in the Au1 (G,H) and BLA (I,J) during conditioned fear retrieval elicited by the 2 kHz tone. Mean ± SEM, n = 6, independent samples *t*-test. $*p < 0.05$, $**p < 0.01$. AUC, area under the curve; Con, control group; F, fluorescence signal value; F_0, baseline fluorescence signal value.

and BLA neurons in the MF&MW group compared with controls (Fig. 6C–F). This reduction was not observed during freezing induced by the non-paired 2 kHz tone in the absence of electric shock, where calcium activity in Au1 and BLA neurons did not differ significantly between groups (Fig. 6G–J). Furthermore, calcium activity in Au1 and BLA

neurons remained unchanged at 6 h after EMF exposure regardless of whether 12 kHz or 2 kHz auditory stimuli were presented (**Supplementary Fig. 5**).

These results indicate that EMF exposure does not affect stimulus-locked auditory encoding in the Au1–BLA circuit but selectively reduces circuit engagement during the expression of conditioned fear. The observed decrease in calcium activity is therefore associated with altered state-dependent recruitment of the Au1–BLA circuit during fear expression, rather than disruption of initial sensory processing or memory acquisition.

3.5 Modulation of Au1 CaMKII-expressing Neurons Alters Conditioned Fear Memory Retrieval in Mice Exposed to EMF

Glutamate is a neurotransmitter involved in memory encoding [30,31] and is closely associated with fear memory [23]. Isler *et al*. [32] found that patients with tinnitus had reduced glutamate levels in the Au1 brain region. Nomura *et al*. [33] used optogenetic technology to inhibit glutamatergic neurons in the Au1, resulting in the impairment of fear memory and memory retrieval in mice. These findings suggest that glutamatergic neurons in the Au1 may play a critical role in conditioned fear memory. This study used chemogenetic manipulation combined with conditioned fear behavioral tests to examine the functional involvement of Au1 excitatory neurons in EMF-associated changes in conditioned fear retrieval. AAV-CaMKII-hM3D(Gq)/hM4D(Gi) containing the glutamatergic neuron-specific promoter CaMKII was injected into the Au1, and clozapine-N-oxide (CNO) was administered via intraperitoneal injection to selectively regulate glutamatergic neurons in the Au1. The "ON" condition refers to chemogenetic activation of Au1 CaMKII-expressing neurons, whereas the "OFF" condition refers to chemogenetic inhibition of the same neuronal population.

The changes in percentage of freezing time during the conditioned fear memory test phase in mice following EMF exposure were analyzed (Fig. 7A). Seven days after EMF exposure, the percentage of freezing time in the MF&MW-NS group was significantly lower than that in the Con-NS group and Con-ON group when paired with a 12 kHz sound stimulus (Fig. 7B,E), whereas it was higher in the MF&MW-NS group than in the Con-NS and Con-ON groups when paired with a 2 kHz sound stimulus (Fig. 7C,F). The ratio of 2:12 kHz freezing time also increased after EMF exposure (Fig. 7D,G). These results were consistent with those of the previous conditioned fear memory behavioral test, and confirmed that EMF exposure can impair conditioned fear memory in mice.

Notably, following chemogenetic activation of Au1 glutamatergic neurons, the percentage of freezing time in the MF&MW-ON group was significantly higher than that in the MF&MW-NS group mice when exposed to 12 kHz stimulus (Fig. 7B), whereas the percentage of freezing time in the MF&MW-ON group mice was significantly lower than that in the MF&MW-NS group mice when exposed to a 2 kHz stimulus (Fig. 7C), and the ratio of 2:12 kHz freezing time was significantly lower in the MF&MW-ON group than in the MF&MW-NS group (Fig. 7D).

However, following inhibition of Au1 glutamatergic neurons, the percentage of freezing time in the MF&MW-NS, MF&MW-OFF, and Con-OFF groups was significantly lower than that in the Con-NS group when exposed to 12 kHz stimulus (Fig. 7E), whereas the percentage of freezing time (Fig. 7F) and the ratios of 2:12 kHz freezing time (Fig. 7G) ratio were significantly higher in the MF&MW-NS, MF&MW-OFF, and Con-OFF groups than in the Con-NS group when exposed to 2 kHz stimulus.

These results indicate that chemogenetic modulation of Au1 CaMKII-expressing neurons is associated with bidirectional changes in conditioned fear expression following EMF exposure. Together, these findings support the functional involvement of Au1 CaMKII-expressing neurons in the modulation of conditioned fear expression under EMF exposure conditions, rather than serving as definitive evidence of cell-type exclusive causality.

3.6 Chemogenetic Activation of Au1 CaMKII-expressing Neurons is Associated With Increased Calcium Activity in BLA Neurons of Mice Exposed to EMF

To further examine the functional relationship between Au1 neuronal activity and BLA dynamics during conditioned fear retrieval, we combined chemogenetic manipulation with genetically encoded calcium imaging to assess changes in BLA neuronal calcium activity following EMF exposure. Seven days after EMF exposure, during presentation of the 12 kHz sound triggered mouse freezing behavior, calcium activity in BLA neurons was significantly higher in the MF&MW-ON group than in the MF&MW-NS group (Fig. 8A,B). In contrast, during presentation of the 2 kHz tone, no significant difference in BLA calcium activity was observed between the MF&MW-ON and MF&MW-NS groups (Fig. 8C,D). These findings indicate that chemogenetic activation of Au1 CaMKII-expressing neurons is associated with a partial restoration of BLA neuronal calcium activity following EMF exposure, supporting a functional link between Au1 activity and BLA engagement during conditioned fear retrieval. After EMF exposure, activation of Au1 glutamatergic neurons in the brain region only increased the calcium activity in BLA neurons after 12 kHZ sound signals, but not after 2 kHz sound signals, possibly because the microcircuits in the BLA mainly encode aversive stimuli [34–36]. These findings suggest that coordinated activity between Au1 and BLA is associated with modulation of conditioned fear memory retrieval following EMF exposure.

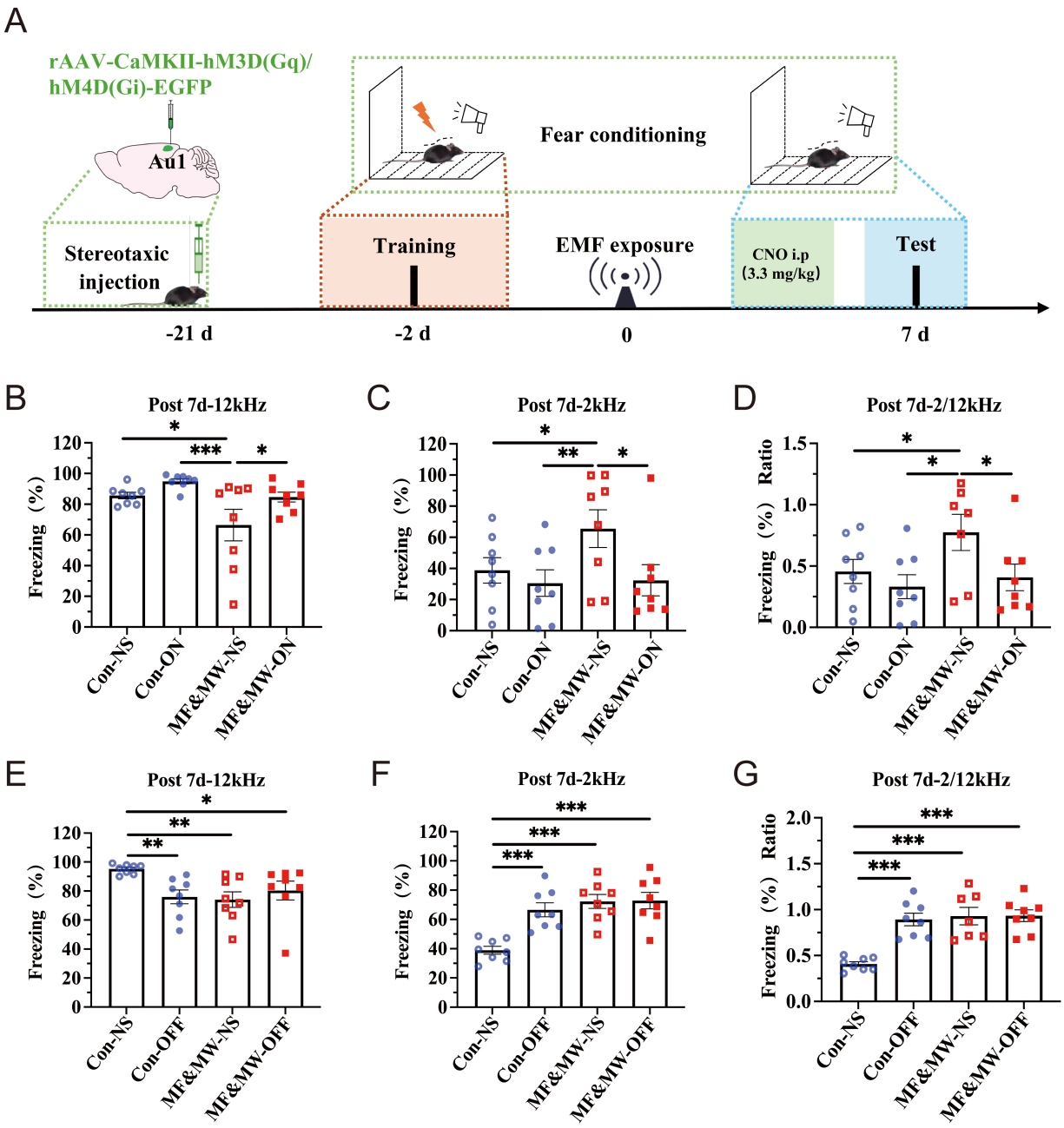

Fig. 7. Chemogenetic modulation of Au1 CaMKII-expressing neurons alters conditioned fear memory retrieval in mice following electromagnetic field exposure. (A) Flowchart of the chemogenetic-based conditioned fear memory experiment. (B–D) Following chemogenetic activation of Au1 CaMKII-expressing neurons, the percentage of freezing time response to 12 kHz (B) and 2 kHz (C) sound stimulus, and the ratio of 2:12 kHz (D) in mice. (E–G) Following chemogenetic inhibition of Au1 CaMKII-expressing neurons, the percentage of freezing time response to 12 kHz (E) and 2 kHz (F) sound stimulus, and the ratio of 2:12 kHz (G) in mice. Mean ± SEM, n = 8. Two-way ANOVA. *$p < 0.05$, **$p < 0.01$, ***$p < 0.001$. Con, control group; MF, static magnetic field exposure group; MF&MW, combined static magnetic field and microwave exposure group; MW, microwave exposure group; NS, normal saline; ON, chemogenetic activation of Au1 CaMKII-expressing neurons; OFF, chemogenetic inhibition of Au1 CaMKII-expressing neurons.

3.7 Activation of Au1 CaMKII-expressing Neurons is Linked to Decreased Cholinergic Signaling in the BLA After EMF Exposure

A neural network consists of intricate neurons interconnected via synapses. Glutamatergic neurons are the primary presynaptic neurons, and Au1 glutamatergic neurons can serve as auditory input neurons. In addition, GABAergic neurons and cholinergic neurons are involved in the acquisition and expression of memory. To explore potential downstream neuronal populations associated with Au1-

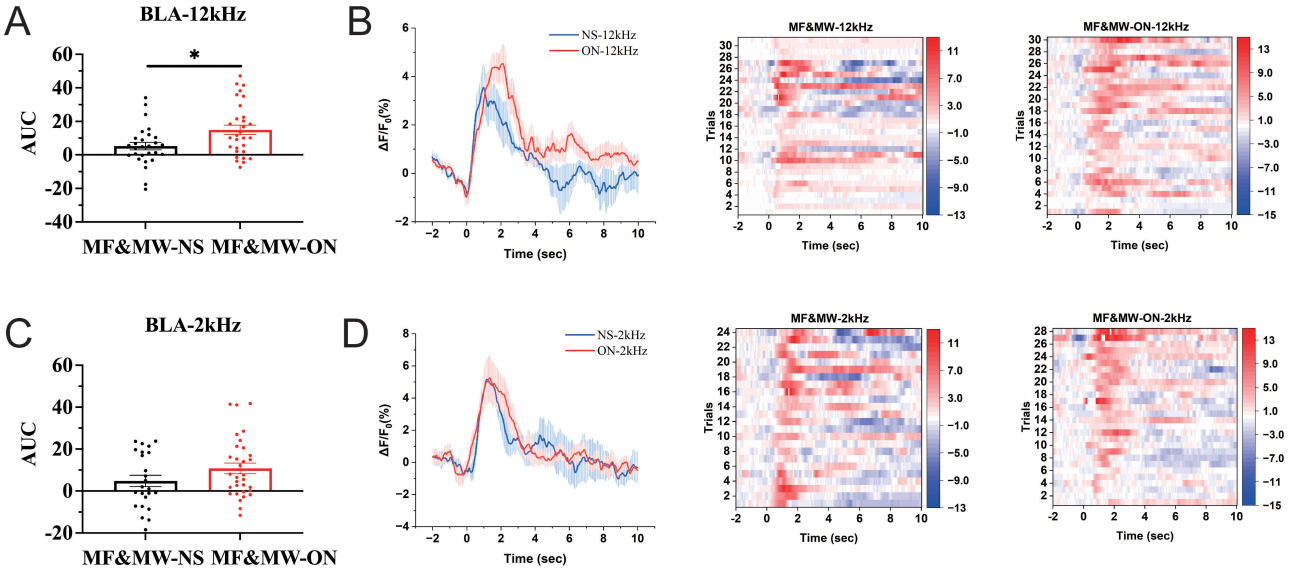

Fig. 8. Activation of Au1 CaMKII-expressing neurons is associated with increased calcium activity in BLA neurons after electromagnetic field exposure. (A,B) Under EMF exposure, following chemogenetic activation of Au1 CaMKII-expressing neurons, AUC analysis (A), mean $\Delta F/F_0$ traces and corresponding heat maps (B) of calcium signals in the BLA during presentation of the 12 kHz conditioned tone. (C,D) Under EMF exposure, AUC analysis (C), mean $\Delta F/F_0$ traces and corresponding heat maps (D) of calcium signals in the BLA during presentation of the 2 kHz tone. Mean ± SEM, N = 6, independent samples *t*-test. $*p < 0.05$. Au1, primary auditory cortex; AUC, area under the curve; BLA, basolateral amygdala; MF&MW, combined static magnetic field and microwave exposure group; NS, normal saline; ON, chemogenetic activation of Au1 glutamatergic neurons.

BLA circuit modulation following EMF exposure, neuronal activity in cholinergic and GABAergic neurons within the BLA was examined using immunofluorescence labeling of c-Fos in combination with cell-type–specific markers (ChAT and GAD67) (Fig. 9A–D).

Quantitative immunofluorescence analysis revealed that, 7 days after EMF exposure, the MF&MW-NS group exhibited both a significantly increased cholinergic activity index—calculated as the ratio of c-Fos–positive area to ChAT-positive area—and an enhanced spatial correlation between ChAT and c-Fos expression in the BLA, compared with the Con-NS and MF&MW-ON groups (Fig. 9E,F). These findings indicate elevated activation and tighter functional coupling of cholinergic neurons in the BLA following EMF exposure. Notably, chemogenetic activation of Au1 CaMKII-expressing neurons significantly attenuated both the increase in cholinergic activity and the ChAT–c-Fos correlation, suggesting that Au1 CaMKII-expressing neuronal activation modulates EMF-associated alterations in BLA cholinergic neuronal activity.

By contrast, the activity index derived from GAD67-positive neurons did not differ significantly among groups (Fig. 9G,H). This suggests that GABAergic neuronal activity in the BLA was not detectably altered by EMF exposure or by Au1 CaMKII-expressing neuronal activation under the present experimental conditions.

4. Discussion

With the rapid advancements in electrical science and technology, the likelihood of public exposure to EMF, ranging from magnetic fields to microwaves, is increasing. The brain is one of the most sensitive target organs affected by EMF, and EMF exposure can lead to neurobehavioral abnormalities, such as impaired cognitive ability and attention [37,38]. Under certain conditions, exposure to static magnetic fields or microwaves can cause a decline in learning abilities and acquisition of memory in mice [39–41]. However, the effects of static magnetic fields and microwave exposure on conditioned fear memory, particularly at the circuit level, have remained largely unexplored.

In the present study, a classical auditory fear conditioning paradigm was used to examine the behavioral consequences of exposure to static magnetic fields and microwaves, either alone or in combination. Our behavioral results indicate that combined EMF exposure is associated with a reduction in conditioned fear memory retrieval, with the most pronounced behavioral effect observed at 7 days after exposure. Importantly, because EMF exposure was applied after establishing fear conditioning, the observed behavioral changes are more appropriately interpreted as alterations in the retrieval of conditioned fear memory, rather than deficits in memory acquisition or initial formation. While extinction processes may be engaged, the immediate reduction in freezing at the 7-day time point (the first major test post-exposure) likely reflects a retrieval deficit, as ex-

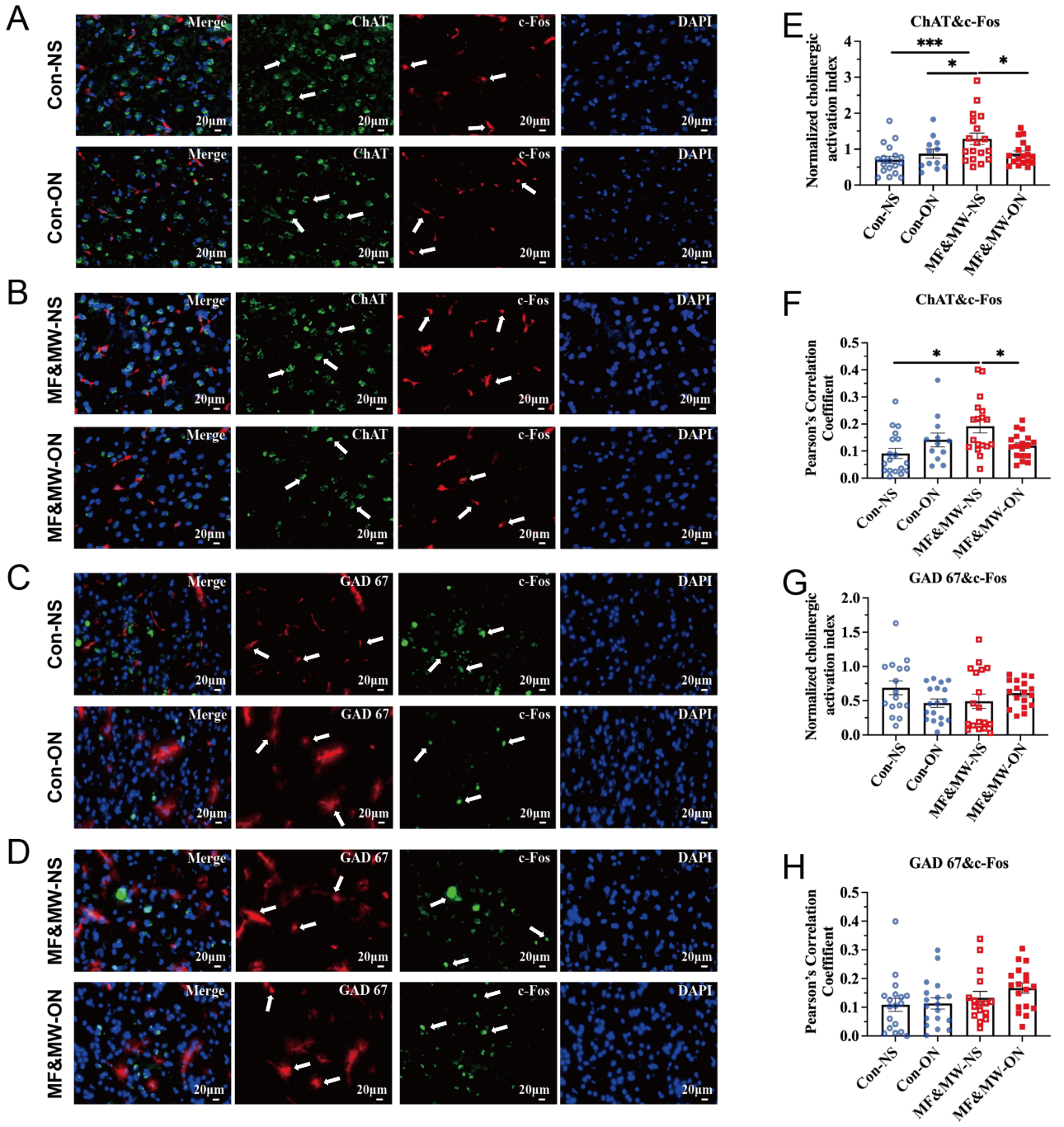

Fig. 9. Changes in cholinergic and GABAergic neuronal activity in the BLA associated with activation of Au1 CaMKII-expressing neurons after electromagnetic field exposure. (A,B) Representative images of ChAT and c-Fos expression in the BLA of mice in the Con-NS and Con-ON groups (A), and the MF&MW-NS and MF&MW-ON groups (B). (C,D) Representative images of GAD 67 and c-Fos expression in the BLA of mice in the Con-NS and Con-ON groups (C), and the MF&MW-NS and MF&MW-ON groups (D). (E) Quantification of cholinergic activity index, calculated as the ratio of c-Fos-positive area to ChAT-positive area (Area-c-Fos/Area-ChAT). (F) Quantification of the Pearson's correlation coefficient reflecting the spatial association between ChAT-positive area and c-Fos-positive area. (G) Quantification of GABAergic activity index, calculated as the ratio of c-Fos-positive area to GAD67-positive area (Area-c-Fos/Area-GAD67). (H) Quantification of the Pearson's correlation coefficient reflecting the spatial association between GAD67-positive area and c-Fos-positive area in the BLA. Mean ± SEM, n = 6, Two-way ANOVA. *$p < 0.05$, ***$p < 0.001$. White arrows indicate cells positive for the respective markers (c-Fos, ChAT, or GAD67). Scale bars: 20 μm (A–D).

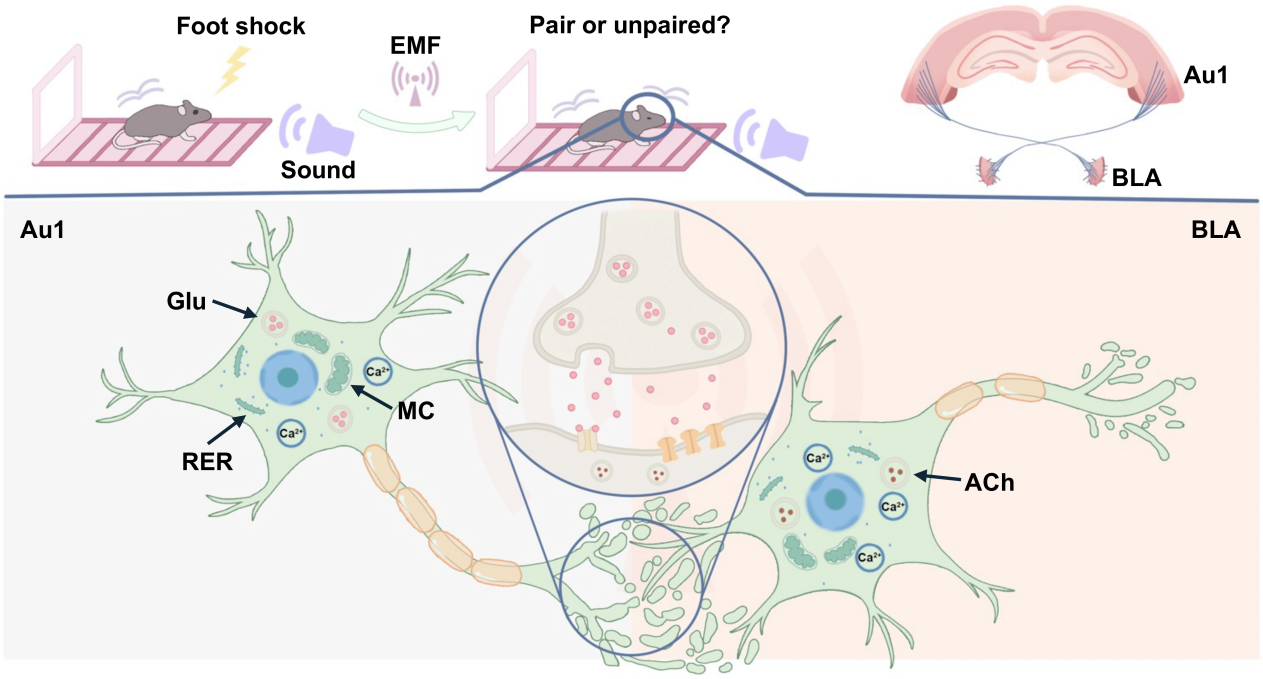

Fig. 10. The role of the primary auditory cortex-basolateral amygdala circuit in the decline of conditioned fear memory retrieval in mice exposed to electromagnetic fields. Exposure to EMF is associated with reduced conditioned fear memory expression in mice, accompanied by decreased calcium activity in neurons of both Au1 and BLA. Histopathological alterations in both regions may contribute to the behavioral disorder. Notably, Au1 CaMKII-expressing neurons are functionally involved in the modulation of conditioned fear memory expression. Furthermore, cholinergic neurons in the BLA may represent sensitive downstream elements within the Au1-BLA circuit, showing altered engagement under EMF exposure conditions. EMF, electromagnetic fields; Glu, Glutamate; RER, Rough endoplasmic reticulum; MC, mitochondrion; ACh, Acetylcholine.

tinction learning typically requires repeated non-reinforced trials to manifest. Because the conditioned stimulus in this study was auditory, we considered whether the reduced freezing responses could be influenced by peripheral hearing alterations. ABR thresholds were unchanged across all exposure groups at 7 days post-exposure, indicating preserved auditory nerve and brainstem function. In addition, DPOAE amplitudes did not differ significantly among exposure groups, indicating intact outer hair cell function. Together, these findings suggest that the behavioral alterations observed following EMF exposure are unlikely to be attributable to peripheral auditory dysfunction.

The execution of learning and memory functions in the central nervous system relies on key constituent structures, including neurons and synapses [42,43]. Among these, synaptic plasticity is a well-studied memory model [44]. Synapses are indispensable neural circuit nodes for learning and memory formation [42,45]. Synaptic plasticity is considered the primary cellular mechanism underlying learning and memory, which explains how experiences are encoded into stable memory traces within neural circuits [45]. Synaptic plasticity in the Au1 can distinguish different types of auditory stimuli [13], and neurons in the BLA play a key role in the formation of fear memory [9]. Previous studies have demonstrated that Au1-BLA interactions contribute to the formation and expression of conditioned fear memory. Consistent with this framework, the present study focused on the Au1-BLA circuit as a candidate pathway through which EMF exposure may modulate fear-related behaviors.

Morphological analyses reveal subtle but consistent changes in neuronal and synaptic features within both Au1 and BLA following EMF exposure. In parallel, viral tracing experiments indicated a reduction in projection-consistent labeling density along the Au1-BLA pathway after combined EMF exposure. Rather than reflecting a definitive loss of anatomical connectivity, these changes are more conservatively interpreted as alterations in the structural integrity, density, or functional state of Au1-BLA projections, which is consistent with the known anatomical organization of cortico-amygdala pathways that are composed of fine, sparsely distributed axons with diffuse terminal fields rather than large bundled fiber tracts [46–49]. Together, these findings suggest that EMF exposure may weaken the effective coupling within the Au1-BLA circuit, thereby contributing to reduced expression of conditioned fear responses. Importantly, these changes do not indicate a loss of macroscopic axonal tracts or a disruption of gross anatomical connectivity between Au1 and the BLA. At the mechanistic level, EMF exposure is more likely to influence

synaptic integrity, axonal terminal maintenance, or activity-dependent labeling efficiency rather than inducing large-scale axonal degeneration. Consistent with this view, ultrastructural abnormalities observed in Au1 and BLA neurons, together with reduced calcium activity and altered neuromodulatory signaling, may contribute to weakened functional coupling within the Au1-BLA circuit without gross anatomical disconnection.

Neuronal calcium signaling is widely recognized as an important link between synaptic activity and plasticity-related processes underlying learning and memory [50–52]. In the present study, calcium imaging revealed a reduction in neuronal calcium activity in both Au1 and BLA following EMF exposure, most notably during the retrieval phase of conditioned fear. Moreover, analyses aligned to the onset of auditory stimulation did not reveal differences in stimulus-evoked calcium responses between experimental and control groups, suggesting that basic auditory processing and initial cue encoding were largely preserved. In contrast, reduced calcium activity became evident during freezing-associated periods, indicating that EMF exposure preferentially alters neural activity during fear retrieval rather than broadly disrupting sensory processing or memory acquisition. Together, these findings suggest that EMF exposure is associated with reduced engagement of the Au1-BLA circuit in a behavior-dependent manner, with alterations in neural activity emerging during the maintenance of conditioned fear rather than as a generalized suppression of circuit excitability.

In the brain, the vast majority of excitatory and glutamatergic neurons express CaMKII, and CaMKII-expressing excitatory neurons are crucial for the formation of learning and memory [53]. Glutamatergic neurons in the Au1 participate in sound discrimination [54–56]. When a sound is paired with another stimulus, Au1 glutamatergic neurons undergo specific changes [57]. This study demonstrated that chemogenetic activation of Au1 CaMKII-expressing neurons attenuated the reduction in conditioned fear memory retrieval observed after EMF exposure, whereas chemogenetic inhibition of Au1 CaMKII-expressing neurons was associated with a further reduction in conditioned fear memory retrieval in mice. Notably, chemogenetic activation of Au1 CaMKII-expressing neurons partially restored calcium activity in BLA neurons during presentation of aversive auditory cues, consistent with a functional coupling between Au1 excitatory output and BLA neuronal activity during aversive cue processing under EMF exposure conditions. These observations support the view that Au1 glutamatergic neurons play a modulatory role in maintaining fear memory retrieval following EMF exposure, likely through their influence on downstream BLA circuits.

Presynaptic excitatory glutamatergic neurons, as auditory input neurons, exhibit enhanced synaptic plasticity of excitatory projection neurons in conditioned fear responses [58]. Wolff *et al*. [59] demonstrated that the conditioned fear memory process is dynamically regulated through the specific activation of multiple inhibitory microcircuits in the BLA region. Both cholinergic and GABAergic neurons in the BLA play roles in the fear memory process [60–62], and the two types of neurons may interact within microcircuits [63]. For EMF exposure, the neuronal types involved in the conditioned fear memory remain unclear. To further explore potential downstream cellular targets within the BLA, we examined activity-dependent c-Fos expression in combination with cell-type-specific markers for cholinergic (ChAT) and GABAergic (GAD67) neurons. Under EMF exposure conditions, increased c-Fos expression was preferentially associated with ChAT-positive neurons in the BLA. Notably, chemogenetic activation of Au1 CaMKII-expressing neurons attenuated this cholinergic-related activity pattern. In contrast, no significant changes were observed in c-Fos association with GAD67-positive neurons across experimental conditions. Together, these findings indicate that EMF exposure and Au1-BLA circuit modulation are associated with differential patterns of activity-related marker engagement within BLA neuronal subtypes, with cholinergic-associated measures showing greater sensitivity under the present experimental conditions. Rather than indicating selective suppression or activation of a single neuronal population, these results are consistent with a model in which Au1 glutamatergic input modulates fear-related activity patterns in the BLA through preferential association with cholinergic-related activity within existing microcircuit frameworks.

In the present study, alterations in conditioned fear memory following combined EMF exposure are consistently accompanied by changes in the functional state of the Au1-BLA pathway. Behavioral deficits were observed alongside reduced neuronal activity and weakened projection-related signals, suggesting that EMF exposure interferes with the normal engagement of this circuit during fear memory expression. Importantly, chemogenetic activation of Au1 CaMKII-expressing neurons partially restored both behavioral performance and BLA neuronal activity, suggesting that reduced Au1 excitatory drive may partly contribute to the observed decline in fear memory retrieval. Although viral tracing revealed changes in projection-associated labeling, these findings should not be interpreted as evidence of a permanent loss of anatomical connectivity. Rather, the data are more consistent with dynamic, activity-dependent modulation of the Au1-BLA circuit. In addition, the absence of a DREADD-negative group receiving CNO represents a limitation of the present study, and therefore potential DREADD-independent effects of CNO cannot be entirely excluded [64,65]. Together, these observations support the view that EMF exposure affects conditioned fear memory primarily by altering circuit function rather than by inducing irreversible structural damage. Further studies focusing on synapse-level plasticity

and cell-type-specific circuit dynamics will be necessary to clarify how these functional changes are established and maintained.

Several limitations should be considered when interpreting these findings. The behavioral paradigm mainly assessed conditioned fear memory retrieval and expression, without directly distinguishing among different stages of memory processing, such as acquisition, consolidation, extinction, or reconsolidation. As the experimental paradigm did not include repeated testing necessary to evaluate other memory stages, such as extinction or reconsolidation, these processes were not assessed in the present study. In addition, although changes in neuronal activity and circuit dynamics within the Au1–BLA pathway were observed, the role of cholinergic signaling was not directly examined. Immunofluorescence results for ChAT suggest a possible involvement of cholinergic neurons; however, this evidence remains indirect. Further studies using cell-type-specific approaches are needed to determine whether cholinergic activity contributes causally to the observed alterations in fear memory. Finally, the analyses in this study were mainly based on population-level measurements and therefore may not fully capture cell-type-specific or microcircuit-level mechanisms. Future work will be required to clarify how different neuronal subtypes, including cholinergic neurons, contribute to EMF-induced changes in fear-related neural circuits.

5. Conclusions

In summary, this study focused on the Au1-BLA circuit and examined the effects of combined static magnetic field and microwave exposure on conditioned fear memory retrieval in mice, together with the underlying regulatory mechanisms (Fig. 10). The figure was generated with Adobe Illustrator 2024 (Adobe Inc., San Jose, CA, USA). Our results demonstrate that combined EMF exposure is associated with a reduction in conditioned fear memory expression, accompanied by alterations in Au1-BLA circuit activity and projection-related signaling. These findings provide new experimental evidence for understanding the biological effects of EMF exposure on brain function and may be informative for evaluating the neurobiological implications of EMF exposure and for guiding future experimental studies. Given that fear overgeneralization and persistence are characteristic features of PTSD, our findings on the Au1-BLA circuit may contribute to a more refined understanding of the neural substrates underlying maladaptive fear responses at both conceptual and circuit-mechanistic levels. However, these findings are not intended to be directly extrapolated to clinical conditions. Further studies will be required to elucidate the detailed neurobiological mechanisms underlying EMF-induced effects, particularly at the levels of microcircuit organization and cell-type-specific regulation within the BLA.

Abbreviations

Au1, primary auditory cortex; BLA, basolateral amygdala; CNO, clozapine-N-oxide; EMF, electromagnetic field; F, fluorescence signal value; F_0, baseline fluorescence signal value; MF, static magnetic field exposure group; MF&MW, combined static magnetic field and microwave exposure group; MW, microwave exposure group; NS, normal saline; ON, chemogenetic activation of Au1 CaMKII-expressing neurons; OFF, chemogenetic inhibition of Au1 CaMKII-expressing neurons; PTSD, posttraumatic stress disorder.

Availability of Data and Materials

The raw data generated in this study (including conditioned fear memory behavioral data, genetically encoded calcium imaging data, and histopathological data of the primary auditory cortex-basolateral amygdala (Au1-BLA) circuit tissues) are available from the corresponding author (Yang Li and Hongyan Zuo) upon reasonable request.

Author Contributions

ZC designed the study, performed data acquisition and analysis, and drafted and revised the manuscript. YLI and HZ contributed to study design and data analysis, and revised the manuscript. LS, MY, CC, SJ, YH, YJL, and XZ performed the experiments and contributed to data acquisition. All authors contributed to editorial revisions of the manuscript. All authors read and approved the final manuscript. All authors have participated sufficiently in the work and agreed to be accountable for all aspects of the work.

Ethics Approval and Consent to Participate

All animal procedures were approved by the Institutional Animal Care and Use Committee of the Beijing Institute of Radiation Medicine (Protocol No. IACUC-DWZX-2021-685). This study was conducted strictly in accordance with relevant ethical guidelines, including the National Institutes of Health Guide for the Care and Use of Laboratory Animals.

Acknowledgment

The authors would like to thank all individuals who provided technical support for this study.

Funding

This study was supported by Chengde Medical University Discipline Construction Funds.

Conflict of Interest

The authors declare no conflict of interest.

Supplementary Material

Supplementary material associated with this article can be found, in the online version, at https://doi.org/10.31083/JIN48640.

References

[1] International Commission on Non-Ionizing Radiation Protection (ICNIRP). Guidelines for Limiting Exposure to Electromagnetic Fields (100 kHz to 300 GHz). Health Physics. 2020; 118: 483–524. https://doi.org/10.1097/HP.0000000000001210.

[2] International Commission on Non-Ionizing Radiation Protection (ICNIRP). Guidelines on limits of exposure to static magnetic fields. Health Physics. 2009; 96: 504–514. https://doi.org/10.1097/01.HP.0000343164.27920.4a.

[3] Broom KA, Findlay R, Addison DS, Goiceanu C, Sienkiewicz Z. Early-Life Exposure to Pulsed LTE Radiofrequency Fields Causes Persistent Changes in Activity and Behavior in C57BL/6 J Mice. Bioelectromagnetics. 2019; 40: 498–511. https://doi.org/10.1002/bem.22217.

[4] Kim JH, Lee CH, Kim HG, Kim HR. Decreased dopamine in striatum and difficult locomotor recovery from MPTP insult after exposure to radiofrequency electromagnetic fields. Scientific Reports. 2019; 9: 1201. https://doi.org/10.1038/s41598-018-37874-z.

[5] Bagheri Hosseinabadi M, Khanjani N, Ebrahimi MH, Haji B, Abdolahfard M. The effect of chronic exposure to extremely low-frequency electromagnetic fields on sleep quality, stress, depression and anxiety. Electromagnetic Biology and Medicine. 2019; 38: 96–101. https://doi.org/10.1080/15368378.2018.1545665.

[6] Dehghani Z, Mahdavi SM, Modarresi Chahardehi A, Mansouri V, Jahani Sherafat S. The Effect of 2.45 GHz Electromagnetic Fields on Fear Memory Extinction in Male Rats. Journal of Lasers in Medical Sciences. 2022; 13: e52. https://doi.org/10.34172/jlms.2022.52.

[7] McKay BE, Persinger MA, Koren SA. Exposure to a theta-burst patterned magnetic field impairs memory acquisition and consolidation for contextual but not discrete conditioned fear in rats. Neuroscience Letters. 2000; 292: 99–102. https://doi.org/10.1016/s0304-3940(00)01437-3.

[8] Izquierdo I, Furini CRG, Myskiw JC. Fear Memory. Physiological Reviews. 2016; 96: 695–750. https://doi.org/10.1152/physrev.00018.2015.

[9] Zhang X, Kim J, Tonegawa S. Amygdala Reward Neurons Form and Store Fear Extinction Memory. Neuron. 2020; 105: 1077–1093.e7. https://doi.org/10.1016/j.neuron.2019.12.025.

[10] Xiao H, Xi K, Wang K, Zhou Y, Dong B, Xie J, *et al*. Restoring the Function of Thalamocortical Circuit Through Correcting Thalamic Kv3.2 Channelopathy Normalizes Fear Extinction Impairments in a PTSD Mouse Model. Advanced Science (Weinheim, Baden-Wurttemberg, Germany). 2024; 11: e2305939. https://doi.org/10.1002/advs.202305939.

[11] Gründemann J. Distributed coding in auditory thalamus and basolateral amygdala upon associative fear learning. Current Opinion in Neurobiology. 2021; 67: 183–189. https://doi.org/10.1016/j.conb.2020.11.014.

[12] Grosso A, Cambiaghi M, Concina G, Sacco T, Sacchetti B. Auditory cortex involvement in emotional learning and memory. Neuroscience. 2015; 299: 45–55. https://doi.org/10.1016/j.neuroscience.2015.04.068.

[13] Wigestrand MB, Schiff HC, Fyhn M, LeDoux JE, Sears RM. Primary auditory cortex regulates threat memory specificity. Learning & Memory (Cold Spring Harbor, N.Y.). 2016; 24: 55–58. https://doi.org/10.1101/lm.044362.116.

[14] Weinberger NM. Physiological memory in primary auditory cortex: characteristics and mechanisms. Neurobiology of Learning and Memory. 1998; 70: 226–251. https://doi.org/10.1006/nlme.1998.3850.

[15] Weinberger NM. Specific long-term memory traces in primary auditory cortex. Nature Reviews. Neuroscience. 2004; 5: 279–290. https://doi.org/10.1038/nrn1366.

[16] Cotovio G, Oliveira-Maia AJ. Functional neuroanatomy of mania. Translational Psychiatry. 2022; 12: 29. https://doi.org/10.1038/s41398-022-01786-4.

[17] Hochgerner H, Singh S, Tibi M, Lin Z, Skarbianskis N, Admati I, *et al*. Neuronal types in the mouse amygdala and their transcriptional response to fear conditioning. Nature Neuroscience. 2023; 26: 2237–2249. https://doi.org/10.1038/s41593-023-01469-3.

[18] Manassero E, Renna A, Milano L, Sacchetti B. Lateral and Basal Amygdala Account for Opposite Behavioral Responses during the Long-Term Expression of Fearful Memories. Scientific Reports. 2018; 8: 518. https://doi.org/10.1038/s41598-017-19074-3.

[19] Kitamura T, Ogawa SK, Roy DS, Okuyama T, Morrissey MD, Smith LM, *et al*. Engrams and circuits crucial for systems consolidation of a memory. Science (New York, N.Y.). 2017; 356: 73–78. https://doi.org/10.1126/science.aam6808.

[20] Wang XJ, Yang XF, Ye YM, Wang YY, Hao YH, Zuo HY, *et al*. Effects of moderate static magnetic field exposure on emotional behavior and brain damage related molecules in mice. Medical Journal of the Chinese People's Liberation Army. 2025; 50: 592–598. (In Chinese)

[21] Tang S, Ye YM, Wang XJ, Yang LL, Zhang X, Wang SX, *et al*. Effects of static field exposure on the depression-like behavior and D2 receptor and DAT expression in hippocampus of rats. Chinese Journal of Stereology and Image Analysis. 2023; 28: 294–301. https://doi.org/10.13505/j.1007-1482.2023.28.03.008. (In Chinese)

[22] Feng ZH, Pan T, He GH, Chang CX, Cui ZL, Yang MY, *et al*. Histopathological changes in secondary visual cortex and enhanced calcium activity in neurons being involved in microwave radiation-induced anxiety-like behavior. Chinese Journal of Radiological Medicine and Protection. 2024; 44: 464–471. (In Chinese)

[23] Johansen JP, Cain CK, Ostroff LE, LeDoux JE. Molecular mechanisms of fear learning and memory. Cell. 2011; 147: 509–524. https://doi.org/10.1016/j.cell.2011.10.009.

[24] Shansky RM, Woolley CS. Considering Sex as a Biological Variable Will Be Valuable for Neuroscience Research. The Journal of Neuroscience: the Official Journal of the Society for Neuroscience. 2016; 36: 11817–11822. https://doi.org/10.1523/JNEUROSCI.1390-16.2016.

[25] Pignatelli M, Ryan TJ, Roy DS, Lovett C, Smith LM, Muralidhar S, *et al*. Engram Cell Excitability State Determines the Efficacy of Memory Retrieval. Neuron. 2019; 101: 274–284.e275. https://doi.org/10.1016/j.neuron.2018.11.029.

[26] Zhao Z, Ma L, Wang Y, Qin L. A comparison of neural responses in the primary auditory cortex, amygdala, and medial prefrontal cortex of cats during auditory discrimination tasks. Journal of Neurophysiology. 2019; 121: 785–798. https://doi.org/10.1152/jn.00425.2018.

[27] Herry C, Johansen JP. Encoding of fear learning and memory in distributed neuronal circuits. Nature Neuroscience. 2014; 17: 1644–1654. https://doi.org/10.1038/nn.3869.

[28] Terranova JI, Yokose J, Osanai H, Marks WD, Yamamoto J, Ogawa SK, *et al*. Hippocampal-amygdala memory circuits govern experience-dependent observational fear. Neuron. 2022; 110: 1416–1431.e1413. https://doi.org/10.1016/j.neuron.2022.01.019.

[29] Yan Y, Song D, Jin Y, Deng Y, Wang C, Huang T, *et al*. ACx-projecting cholinergic neurons in the NB influence the BLA en-

sembles to modulate the discrimination of auditory fear memory. Translational Psychiatry. 2023; 13: 79. https://doi.org/10.1038/s41398-023-02384-8.
[30] Lisman J, Yasuda R, Raghavachari S. Mechanisms of CaMKII action in long-term potentiation. Nature Reviews. Neuroscience. 2012; 13: 169–182. https://doi.org/10.1038/nrn3192.
[31] Bliss TV, Collingridge GL. A synaptic model of memory: long-term potentiation in the hippocampus. Nature. 1993; 361: 31–39. https://doi.org/10.1038/361031a0.
[32] Isler B, von Burg N, Kleinjung T, Meyer M, Stämpfli P, Zölch N, *et al*. Lower glutamate and GABA levels in auditory cortex of tinnitus patients: a 2D-JPRESS MR spectroscopy study. Scientific Reports. 2022; 12: 4068. https://doi.org/10.1038/s41598-022-07835-8.
[33] Nomura H, Hara K, Abe R, Hitora-Imamura N, Nakayama R, Sasaki T, *et al*. Memory formation and retrieval of neuronal silencing in the auditory cortex. Proceedings of the National Academy of Sciences of the United States of America. 2015; 112: 9740–9744. https://doi.org/10.1073/pnas.1500869112.
[34] Gao Y, Gao D, Zhang H, Zheng D, Du J, Yuan C, *et al*. BLA DBS improves anxiety and fear by correcting weakened synaptic transmission from BLA to adBNST and CeL in a mouse model of foot shock. Cell Reports. 2024; 43: 113766. https://doi.org/10.1016/j.celrep.2024.113766.
[35] O'Neill PK, Gore F, Salzman CD. Basolateral amygdala circuitry in positive and negative valence. Current Opinion in Neurobiology. 2018; 49: 175–183. https://doi.org/10.1016/j.conb.2018.02.012.
[36] Hájos N. Interneuron Types and Their Circuits in the Basolateral Amygdala. Frontiers in Neural Circuits. 2021; 15: 687257. https://doi.org/10.3389/fncir.2021.687257.
[37] Zhi WJ, Wang LF, Hu XJ. Recent advances in the effects of microwave radiation on brains. Military Medical Research. 2017; 4: 29. https://doi.org/10.1186/s40779-017-0139-0.
[38] Mumtaz S, Rana JN, Choi EH, Han I. Microwave Radiation and the Brain: Mechanisms, Current Status, and Future Prospects. International Journal of Molecular Sciences. 2022; 23: 9288. https://doi.org/10.3390/ijms23169288.
[39] Saeedi Goraghani M, Ahmadi-Zeidabadi M, Bakhshaei S, Shabani M, Ghotbi Ravandi S, Rezaei Zarchi S, *et al*. Behavioral consequences of simultaneous postnatal exposure to MK-801 and static magnetic field in male Wistar rats. Neuroscience Letters. 2019; 701: 77–83. https://doi.org/10.1016/j.neulet.2019.02.026.
[40] Hao Y, Liu W, Liu Y, Liu Y, Xu Z, Ye Y, *et al*. Effects of Non-thermal Radiofrequency Stimulation on Neuronal Activity and Neural Circuit in Mice. Advanced Science (Weinheim, Baden-Wurttemberg, Germany). 2023; 10: e2205988. https://doi.org/10.1002/advs.202205988.
[41] Li H, Gao Y, Zou Y, Qiao S, Zhi W, Ma L, *et al*. Associations Between a Polymorphism in the Rat 5-HT_{1A} Receptor Gene Promoter Region (rs198585630) and Cognitive Alterations Induced by Microwave Exposure. Frontiers in Public Health. 2022; 10: 802386. https://doi.org/10.3389/fpubh.2022.802386.
[42] Magee JC, Grienberger C. Synaptic Plasticity Forms and Functions. Annual Review of Neuroscience. 2020; 43: 95–117. https://doi.org/10.1146/annurev-neuro-090919-022842.
[43] Alberini CM. Not just neurons: The diverse cellular landscape of learning and memory. Neuron. 2025; 113: 1664–1679. https://doi.org/10.1016/j.neuron.2025.05.005.
[44] Nicoll RA. A Brief History of Long-Term Potentiation. Neuron. 2017; 93: 281–290. https://doi.org/10.1016/j.neuron.2016.12.015.
[45] Hwang FJ, Roth RH, Wu YW, Sun Y, Kwon DK, Liu Y, *et al*. Motor learning selectively strengthens cortical and striatal synapses of motor engram neurons. Neuron. 2022; 110: 2790–2801.e2795. https://doi.org/10.1016/j.neuron.2022.06.006.
[46] Romanski LM, LeDoux JE. Information cascade from primary auditory cortex to the amygdala: corticocortical and corticoamygdaloid projections of temporal cortex in the rat. Cerebral Cortex (New York, N.Y.: 1991). 1993; 3: 515–532. https://doi.org/10.1093/cercor/3.6.515.
[47] McDonald AJ. Cortical pathways to the mammalian amygdala. Progress in Neurobiology. 1998; 55: 257–332. https://doi.org/10.1016/s0301-0082(98)00003-3.
[48] Winnubst J, Bas E, Ferreira TA, Wu Z, Economo MN, Edson P, *et al*. Reconstruction of 1,000 Projection Neurons Reveals New Cell Types and Organization of Long-Range Connectivity in the Mouse Brain. Cell. 2019; 179: 268–281.e13. https://doi.org/10.1016/j.cell.2019.07.042.
[49] Hintiryan H, Bowman I, Johnson DL, Korobkova L, Zhu M, Khanjani N, *et al*. Connectivity characterization of the mouse basolateral amygdalar complex. Nature Communications. 2021; 12: 2859. https://doi.org/10.1038/s41467-021-22915-5.
[50] He G, Li Y, Deng H, Zuo H. Advances in the study of cholinergic circuits in the central nervous system. Annals of Clinical and Translational Neurology. 2023; 10: 2179–2191. https://doi.org/10.1002/acn3.51920.
[51] Wood A, Karipidis K. Radiofrequency Fields and Calcium Movements Into and Out of Cells. Radiation Research. 2021; 195: 101–113. https://doi.org/10.1667/RADE-20-00101.1.
[52] Brini M, Calì T, Ottolini D, Carafoli E. Neuronal calcium signaling: function and dysfunction. Cellular and Molecular Life Sciences: CMLS. 2014; 71: 2787–2814. https://doi.org/10.1007/s00018-013-1550-7.
[53] Yasuda R, Hayashi Y, Hell JW. CaMKII: a central molecular organizer of synaptic plasticity, learning and memory. Nature Reviews. Neuroscience. 2022; 23: 666–682. https://doi.org/10.1038/s41583-022-00624-2.
[54] Weinberger NM. New perspectives on the auditory cortex: learning and memory. Handbook of Clinical Neurology. 2015; 129: 117–147. https://doi.org/10.1016/B978-0-444-62630-1.00007-X.
[55] Schreiner CE, Polley DB. Auditory map plasticity: diversity in causes and consequences. Current Opinion in Neurobiology. 2014; 24: 143–156. https://doi.org/10.1016/j.conb.2013.11.009.
[56] Francis NA, Winkowski DE, Sheikhattar A, Armengol K, Babadi B, Kanold PO. Small Networks Encode Decision-Making in Primary Auditory Cortex. Neuron. 2018; 97: 885–897.e886. https://doi.org/10.1016/j.neuron.2018.01.019.
[57] Froemke RC, Merzenich MM, Schreiner CE. A synaptic memory trace for cortical receptive field plasticity. Nature. 2007; 450: 425–429. https://doi.org/10.1038/nature06289.
[58] Lucas EK, Clem RL. GABAergic interneurons: The orchestra or the conductor in fear learning and memory? Brain Research Bulletin. 2018; 141: 13–19. https://doi.org/10.1016/j.brainresbull.2017.11.016.
[59] Wolff SBE, Gründemann J, Tovote P, Krabbe S, Jacobson GA, Müller C, *et al*. Amygdala interneuron subtypes control fear learning through disinhibition. Nature. 2014; 509: 453–458. https://doi.org/10.1038/nature13258.
[60] Lovett-Barron M, Kaifosh P, Kheirbek MA, Danielson N, Zaremba JD, Reardon TR, *et al*. Dendritic inhibition in the hippocampus supports fear learning. Science (New York, N.Y.). 2014; 343: 857–863. https://doi.org/10.1126/science.1247485.
[61] Chhatwal JP, Myers KM, Ressler KJ, Davis M. Regulation of gephyrin and GABAA receptor binding within the amygdala after fear acquisition and extinction. The Journal of Neuroscience: the Official Journal of the Society for Neuroscience. 2005; 25: 502–506. https://doi.org/10.1523/JNEUROSCI.3301-04.2005.
[62] Lin HC, Mao SC, Gean PW. Block of gamma-aminobutyric acid-A receptor insertion in the amygdala impairs extinction

of conditioned fear. Biological Psychiatry. 2009; 66: 665–673. https://doi.org/10.1016/j.biopsych.2009.04.003.

[63] Yuan M, Meyer T, Benkowitz C, Savanthrapadian S, Ansel-Bollepalli L, Foggetti A, *et al*. Somatostatin-positive interneurons in the dentate gyrus of mice provide local- and long-range septal synaptic inhibition. eLife. 2017; 6: e21105. https://doi.org/10.7554/eLife.21105.

[64] Gomez JL, Bonaventura J, Lesniak W, Mathews WB, Sysa-Shah P, Rodriguez LA, *et al*. Chemogenetics revealed: DREADD occupancy and activation via converted clozapine. Science (New York, N.Y.). 2017; 357: 503–507. https://doi.org/10.1126/science.aan2475.

[65] Roth BL. DREADDs for Neuroscientists. Neuron. 2016; 89: 683–694. https://doi.org/10.1016/j.neuron.2016.01.040.